ACCESS
Arctic Climate Change
Economy and Society

SEVENTH FRAMEWORK
PROGRAMME

Project no. 265863

ACCESS

Arctic Climate Change, Economy and Society

Instrument: Collaborative Project

Thematic Priority: Ocean.2010-1 "Quantification of climate change impacts on economic sectors in the Arctic"

D1.82 – Future scenarios for evolution of the observing system for Arctic short-range forecasting

Roger Randriamampianina, Stéphanie Guedj, Máté Mile and Harald Schyberg

Due date of deliverable: **31/08/2014**

Actual submission date: **26/02/2015**

Used Person/months: **12**

Start date of project: **March 1st, 2011** Duration: **48 months**

Organisation name of lead contractor for this deliverable: **Met.no**

Project co-funded by the European Commission within the Seventh Framework Programme (2007-2013)		
Dissemination Level		
PU	Public	X
PP	Restricted to other programme participants (including the Commission Services)	
RE	Restricted to a group specified by the consortium (including the Commission Services)	
CO	Confidential, only for members of the consortium (including the Commission Services)	

Contents

Table of Contents

1 Introduction

In the present report the goal is to identify key factors limiting the monitoring and short-range weather forecasting capabilities, and give a foundation for recommendations for a future cost effective evolution of the Arctic forecasting system. This is important for the safety of operations in the harsh Arctic environment. In an earlier report (Schyberg et al, 2013), we discussed the fact that numerical weather prediction (NWP) forecasting quality decreases towards the Arctic in the Northeast Atlantic region. This was found both in the ECMWF (European Centre for Medium-range Weather Forecast) global model [1] and the High Resolution Limited Area Model (HIRLAM, [3]), which were (and ECMWF is still) operationally in use at the time of the reporting. It was argued that a likely main factor behind this is gaps in the observing system. The network of conventional observations is sparse in the Arctic, in particular coverage of aircraft observations and radiosonde data. It is important to describe the full 3-D initial state of the atmosphere to do good forecasts, and the lack of such upper-air data is a difference from the observing system over land at lower latitudes.

There is good coverage of satellite data from polar-orbiting satellites at high latitudes, where for instance sensors with temperature and moisture sounding capabilities are available, but overall limited coverage in the lower troposphere with satellite information.

We have chosen to do our studies with the so-called HARMONIE-AROME NPW model, wich is presently the operational regional NWP model in Norway. The HIRLAM group now has joined the ALADIN (Aire Limitée Adaptation Dynamic Internationale) consortium [2] and started to develop a common non-hydrostatic high-resolution limited area model of the HARMONIE (Hirlam Aladin Regional Meso-scale Operational NWP In Euromed) (referred as Harmonie hereafter) system. HARMONIE is an numerical weather prediction system, where different meso-scale deterministic and ensemble systems are accessible. In this study we use the meso-scale non-hydrostatic model with the AROME physics (*Seity et al., 2011*) and implemented over the Arctic (referred as AROME-Arctic hereafter).

The impact of observations on the AROME-Arctic meso-scale non-hydrostatic analyses and forecasts is discussed Sections 2 through observing system experiments (OSE). In Section 3 the set-up of observing system simulation experiments (OSSE) is illustrated. In Section 4 summarises and discusses the obtained results.

Significant work on observing system studies and planning of future observation systems have been done in global NWP experiments with coarser resolution than our model. Besides the fact that AROME-Arctic is a system close to what we would use for operational short-range forecasting, it also allows us to focus on local effects of observations in an Arctic domain. This system with 2.5 km horizontal resolution will allow us an assessment of observations in a high-resolution modeling framework. Also global models are expected to evolve towards such resolutions in the future.

The disadvantage with working on a limited-area like this is that in addition to the sensitivity of forecasts to observations through the initial state, there is a dependence on the lateral boundaries througout the model forecast. These lateral boundaries are taken from longer forecasts from a host model, in this case the ECMWF model. Information from observations propagates away, and will only be kept for a limited time inside the domain before the influence of the lateral boundaries take over. In practise this means that the differences between various observation scenarios usually are smaller in such a system than in a global model, and is not increasing with forecast length in the same way we see in global models. Beacuse of this, we may have larger problems in showing statistically significant differences between scenarios.

2 Observing system experiment (OSE)

We have chosen to evaluate and quantify the results of the OSEs with the present model and observing system with several different means. After describing some more details on our system and experiment setup, we present a measure of the impact of the observations on the analysis quality. This measure (so called DFS, see further details below) gives information on the amount of contribution each observation or observation type does to the quality of the analyses the forecasts are started from. This is under the assumption that the information on accuriacies in observations and forecasts which we specify in the assimilation scheme, is correct. Impact on analysis quality is usually strongly correlated with impact on forecast quality, but there is not necessarily a one-to-one relationship, because some types of errors amplify more throughout a forecast than others.

It is therefore also necessary to evaluate the impact on forecasts. This is done first by verifying forecasts with the few observations we have in the area in terms of average statistics. Such statistics weights all events equally, but it is also of interest to evaluate the observation scenarios specifically in high-impact events where good forecasts are really important. This we have done by case studies of cyclone developments. We have finally used a scalar measure of the observing system impact on the forecasts using a norm which is computed based on a particular definition of energy in the atmospheric domain.

All these assessments are based on scenarios using the components of the present Arctic observing system. More detailed evaluations of scenarios for the future observing systems which are not available yet, need to be done with a observation simulation approach, which is described afterwards in Section 3.

2.1 The AROME-Arctic assimilation and forecast system

The characteristics of the AROME-Arctic (using the AROME physical parametrisation) used in this experiment is very similar to one used operationally at MET-Norway. In this experiment we used hourly ECMWF forecasts as lateral boundary conditions (LBC). As default setting in the Harmonie system, a spectral blending of the ECMWF field is used at zero-time step (Vignes, 2011). This is a procedure which blends in the larger-scale structures believed to have a good quality in the ECMWF model, but leaves the smaller-scale structures untouched. The assimilation system includes a surface Optimal Interpolation scheme to update soil moisture content and skin temperature fields, and an upper-air spectral three-dimensional variational (3D-Var) assimilation to analyse wind, temperature, specific humidity and surface pressure fields. Together with the conventional observations (surface, radiosondes, and aircrafts), radiance data (ATOVS – AMSU-A, AMSU-B/MHS; and IASI) are also assimilated. The AROME-Arctic model domain was set up with a same size as the operational MetCoOp model (Meteorological Cooperation for Operational NWP – a cooperation between MET-Norway and the Swedish Meteorological and Hydrological Institute), but suitably rotated to cover the Arctic and also partly the area of interest of MET Norway (*Fig. 1*). The horizontal resolution of model is 2.5 km (with 750x960 grid points) and 65 vertical atmospheric levels ranging from roughly 12m (level 65) till 10 hPa (level 1). 3-hourly cycling is used for better accounting of the available observations. Hence, 8 analyses are performed per day at 00, 03, 06, 09, 12, 15, 18, and 21 UTC, respectively. The performance of the AROME-Arctic model is verified twice a day doing longer integration (48 hours) at 00 and 12 UTC. The recent *cy38h1.1* version of the Harmonie system is used in our experiment.

2.1.1 Satellite radiance data processing

For the satellite radiance data utilization, the version 10 of the RTTOV (radiative transfer for TOVS) model is used (*Matricardi et al.*, 2004). RTTOV uses coefficients calculated by training a regression with a more accurate, but also more computationally demanding, line-by-line radiative transfer model. The IASI radiances are processed using the coefficients

derived from the line-by-line RTM (LBLRTM) (*Clough et al.* 1992; 2005). For radiance data simulation 43 vertical levels are used, ranging from 0.1 – 1013.25 hPa. The microwave radiances are processed at their full resolution in the system according to *Randriamampianina* (2006). The same for IASI radiances, data from all IASI fields of views (FOVs) from all fields of regards (FOR) are used. In this study we followed the suggestions made by *Lindskog et al.* 2012, with respect to the computation and selection of the predictors for radiance bias correction. The "adaptivity" of the variational bias correction (VarBC) scheme (Auligné *et al.*, 2007) was in our setup tuned so that the parameters nbg_AMSUA, nbg_AMSUB, nbg_MHS, and nbg_IASI were set to be 2000 instead of the default value (5000) in the system. Due to the fact that the model top is 10 hPa, the predictors 5 and 6 are not used for radiances bias computation. According to *Lindskog et al.* 2012, we do not use either the predictor 2 in this experiment.

To simulate an operational system and to ensure accounting for a continuous atmospheric flow influence, the coefficients for the VarBC were estimated for the month of November 2013, while the experiments were done for December 2013.

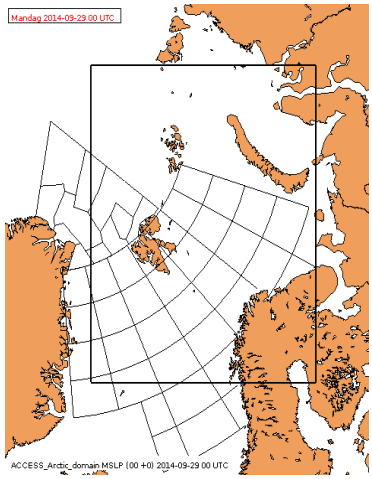

Figure 1. The AROME-Arctic model domain with the "high-sea" MET Norway service/obligation area.

Table 1. Use of observations in the AROME-Arctic. Note, 10m winds are assimilated over sea only.

Type	**Parameter (Channel)**	**Bias Correction**	**Thinning**
TEMP	U, V, T, Q	Only T, using ECMWF tables	No
SYNOP	Z, V10m, U10m	No	Temporal and spatial
DRIBU	Z	No	Temporal and spatial
AIREP	U, V, T	No	25 Km horizontal
AMSU-A	6 to 10	Variational	80 Km horizontal
AMSU-B, MHS	3, 4, 5	Variational	80 Km horizontal
IASI	Channels (see Table 2)	Variational	80 Km horizontal

Table 2. IASI channels assimilated. The central wave number of a channel can be determined using the formula c = (channel -1) x 0.25 + 645.0.

	IASI
Over Sea	38, 51, 63, 85, 104, 109, 167, 173, 180, 185, 193, 199, 205, 207, 212, 224, 230, 236,

	239, 242, 243, 249, 252, 265, 275, 294, 296, 306, 333, 337, 345, 352, 386, 389, 432, 2919, 3008, 3014, 3069, 3087, 3098, 3207, 3228, 3281, 3309, 3322, 3339, 3438, 3442, 3484, 3491, 3499, 3506, 3575, 3582, 3658
Over Land	38, 51, 63, 85, 104, 109, 167, 173, 180, 185, 193, 199, 205, 207, 212, 224, 230, 236, 239, 242, 243, 249, 252, 265, 275, 294, 296, 306, 345, 386, 389, 432, 2919, 3069, 3087, 3098, 3281, 3309, 3339, 3442, 3484, 3491, 3499, 3506, 3575, 3582, 3658, 4032
Over sea ice	51, 63, 85, 87, 104, 109, 167, 173, 180, 185, 193, 199, 205, 207, 212, 224, 239, 265, 275, 294, 306, 2701, 2819, 2910, 2991, 2993, 3002, 3008, 3014, 3027

2.2 The performed experiments

To evaluate the impact of different observations on the AROME-Arctic analyses and forecasts, the following experiments were conducted for a period of 25 days (from 1rst to 25th of December 2013), where the first 4 days were not used due to "warm-up" issues with the system. Hence, data from 5th till 25th were used in the different evaluations (see the Section 3). The following observing system scenarios was run with the system (with corresponding labels):

ARCREF – No assimilation is used. The model starts with an interpolated short-range ECMWF forecast;

ARCSURF – Only surface assimilation is used to update the surface fields. Note, the sea surface temperature are also updated using the ECMWF fields.

ARCCONV – Surface and upper-air analyses are used accounting only the conventional observations;

ARCAIREP – Surface and upper-air analyses are used accounting only the conventional observations without aircraft data;

ARCAMSUAN [1] – Surface and upper-air analyses are used accounting conventional and AMSU-A microwave radiances;

ARCAMSUB – Surface and upper-air analyses are used accounting conventional and AMSU-B/MHS microwave radiances;

ARCATOVN (see footnote 1) – Surface and upper-air analyses are used accounting conventional and ATOVS (AMSU-A and AMSU-B/MHS microwave) radiances;

ARCIASI – Surface and upper-air analyses are used accounting conventional and IASI hiperspectral infrared radiances;

The experiments described and labelled below were performed for few cases only (*see Section 3.4.1 for more details*):

NAAIREPMTEN – A re-run experiment with surface and upper-air assimilation with full observations except aircraft;

NATEMPMTEN – A re-run experiment with surface and upper-air assimilation with full observations except radiosondes;

NASYNOPMTEN – A re-run experiment with upper-air assimilation with full observations except the SYNOP surface data (technically surface assimilation is not possible for this case);

NABUOYMTEN – A re-run experiment with surface and upper-air assimilation with full observations except drifting buoys;

1- N at the end of the experiment name means “new run”. This also means that we had to re-run the experiment to account for more blacklisting of bad channels from certain satellites. The same happened with the run with ATOVS data.

NAAMSUAMTEN – A re-run experiment with surface and upper-air assimilation with full observations except the AMSU-A radiances;

NAAMSUBMTEN – A re-run experiment with surface and upper-air assimilation with full observations except the AMSU-B/MHS radiances;

NAIASIMTEN – A re-run experiment with surface and upper-air assimilation with full observations except the IASI radiances;

2.3 The impact of the observations on the AROME-Arctic analyses and forecasts

2.3.1 The impact of the observations on the analyses

To evaluate the sensitivity of the analysis system (3D-VAR) to the different observations, the degrees of freedom for signal (DFS) is used. The DFS is defined as the derivative of the analysis increments in observation space with respect to the observations used in the analysis system. In practice, it is computed through a randomization technique (*Chapnik et al. 2006*), which reads:

$$DFS = \frac{\partial(\mathbf{H}\mathbf{x}^{\mathbf{a}})}{\partial \mathbf{y}} \approx (\tilde{\mathbf{y}} - \mathbf{y})\mathbf{R}^{-1}\left\{\mathbf{H}(\tilde{\mathbf{x}}^{\mathbf{a}} - \mathbf{x}^{\mathbf{b}}) - \mathbf{H}(\mathbf{x}^{\mathbf{a}} - \mathbf{x}^{\mathbf{b}})\right\}, \quad (1)$$

where $\mathbf{y}$ is the vector of the observations, $\tilde{\mathbf{y}}$ is the vector of perturbed observations, $\mathbf{R}$ is the observation-error covariance matrix, $\mathbf{H}$ is the tangent-linear observation operator for each observation type, $\mathbf{x}^{\mathbf{a}}$ and $\mathbf{x}^{\mathbf{b}}$ are the analysis and the background state, respectively, and $\tilde{\mathbf{x}}^{\mathbf{a}}$ is the analysis produced with perturbed observations. The previous formulation can be applied to any subset of observations.

The absolute DFS represent the information brought into the analyses by the different observation types, in terms of amount, distribution, instrumental accuracy and observation operator definition. They offer an insight to the actual weight given to the observations within the analysis system in terms of self-sensitivity of the observations (i.e. sensitivity at observation location), but do not provide any information on the spatial or crosscorrelations between the observations and the analysis. Relative DFS (DFS normalized by the amount of the observations belonging to a specific subset) provide a theoretical value associated to each observation type, regardless of its actual amount and geographical coverage in the analysis system. DFS as a diagnostic tool has been successfully used in different studies. For example, *Rabier et al. (2002)* used it to perform channel selection on simulated IASI radiances, while *Cardinali et al. (2004), Montmerle et al. (2007)*, and *Randriamampianina et al. (2011)* applied it to study the respective influence of different types of observations in an analysis system. To reduce the interdependency between the initial conditions, for the DFS computation the following times and dates were chosen: 12 UTC for 06.12.2013 and 15.12.2013, and 00 UTC for 10.12.2013 and 19.12.2013. The final DFS values are the mean over the four selected times.

Analysing the results on the sensitivity of the analysis system to different observation types (*Fig 2.*), we can see the importance of the humidity observations. Actually, from conventional observations, only radiosondes humidity is assimilated and from radiances humidity sensitive channels are from AMSU-B/MSH and IASI. The sensitivity of the AROME model assimilation systems to the humidity is also shown over the mid-latitude regions studies (*e.g. Mile et al., 2014*). The satellite observations are the principal sources of information over the Arctic. The more satellite data is included in the scenario, the less is the relative importance of the conventional observation. Although, this more visible only in case of drifting buoys (DRIBU) and less for the other observation types (*Fig 3*).

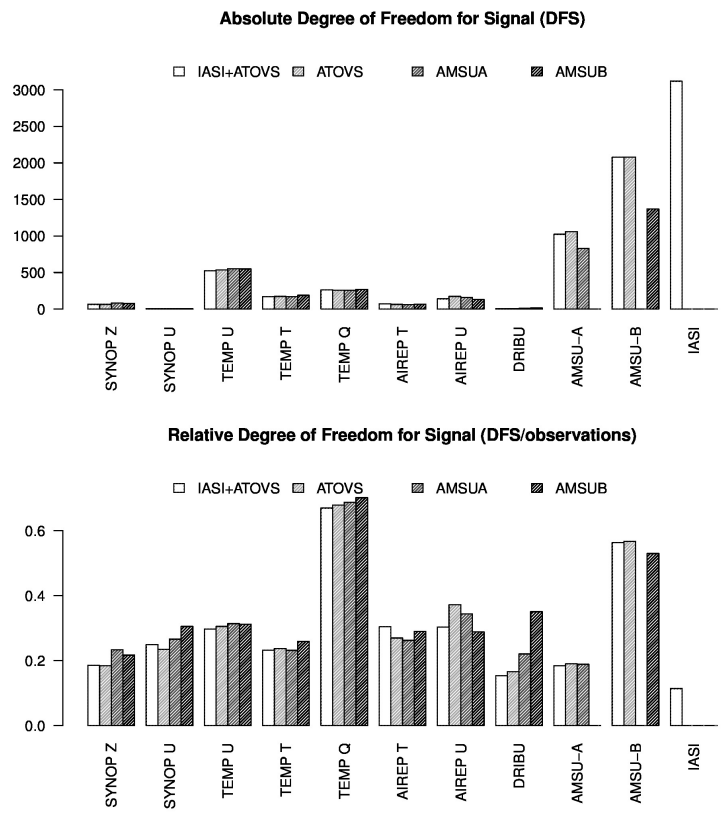

Figure 2. Absolute (top) and relative (bottom) DFS expressing the sensitivity of the analysis system to different observed parameters in use. Where: IASI+ATOVS – conventional data + IASI +ATOVS; ATOVS – conventional data + ATOVS; AMSUA – conventional data + AMSU-A; and AMSUB – conventional data + AMSU-B/MHS.

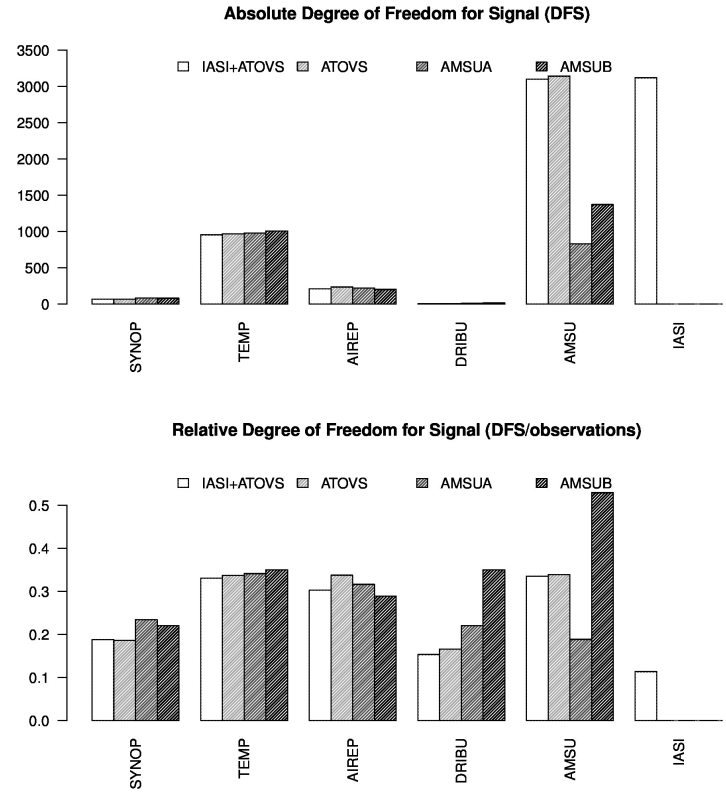

Figure 3. Same as in Fig. 2 but computed for different observation types.

2.4 The impact of the observations on the forecasts

In this Section we discuss the impact of different type of observations on the forecasts of the AROME-Arctic non-hydrostatic meso-scale models. The forecasts are compared with observations (surface and radiosonde). Although, the best choice of verification method would suggest to use independent observations (those which were not used in the assimilation process), the situation over the studied region does have enough observations to fulfil this requirement. So, when analysing the verification results, we need to keep in mind that the evaluation is with respect to the used observations. It should be noted that since we evaluate forecasts where the impact of the observations in the initial state has propagated throughout the area, we do not believe that this is a large limitataion to the confidence we can have in the results. Figure 4 shows the usual verifying surface stations over the AROME-Arctic domain, where most of the stations are over land.

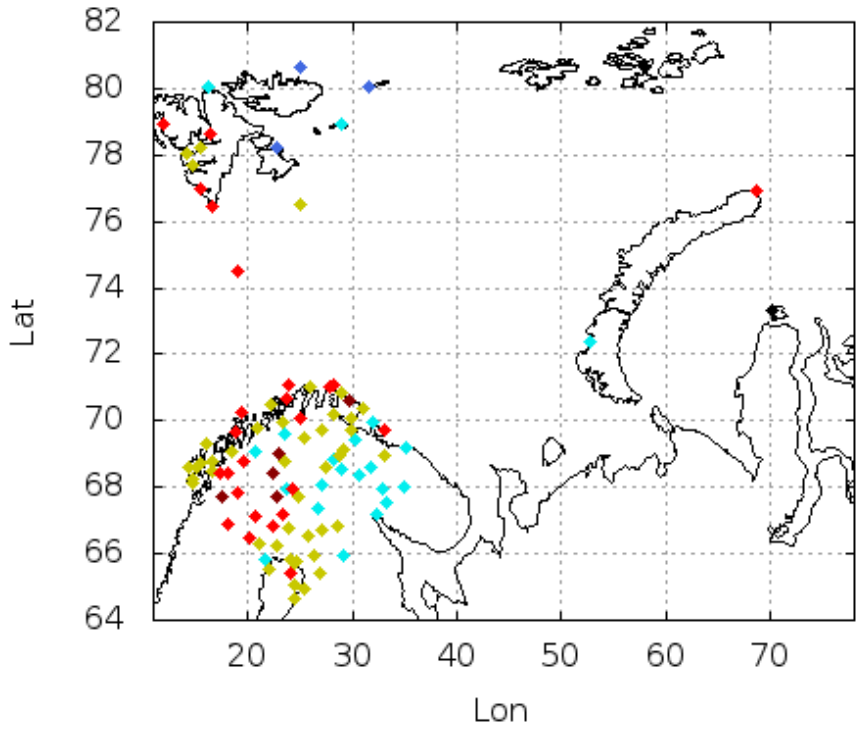

Figure 4. Coloured dots shows the positions of the available verifying stations inside the AROME-Arctic model.

The verification against observations presented in Figures 5-10 shows the following main findings:

1- Without assimilation of observations (at least in the model surface scheme) the HARMONIE-AROME system is not able to provide accurate forecasts, especially in the planetary boundary layer and lower troposphere. This is related to a deficiency coming from the fact that surface information is taken from the ECMWF model which uses a different surface scheme from AROME-Arctic, and this may inevitably result in biases which need to be corrected.

2- The impact of the surface assimilation is large and lasts up to 24 hour for 2m temperature (*Fig. 5.a*), and even longer for the 10m wind (*Fig. 5b*). We can see that for all wind intensity exceedance classes, the impact is clearly positive (all occurance classes in *Fig 5b*). The impact of observation assimilation (surface only or together with upper-air 3D-VAR is significantly positive up to 48 hours forecast, not shown). But, we also observe a negative impact on 2m relative humidity (Fig.5c). The impact of the surface assimilation is affecting also the near-surface/lower part of the troposphere (Fig. 5d).

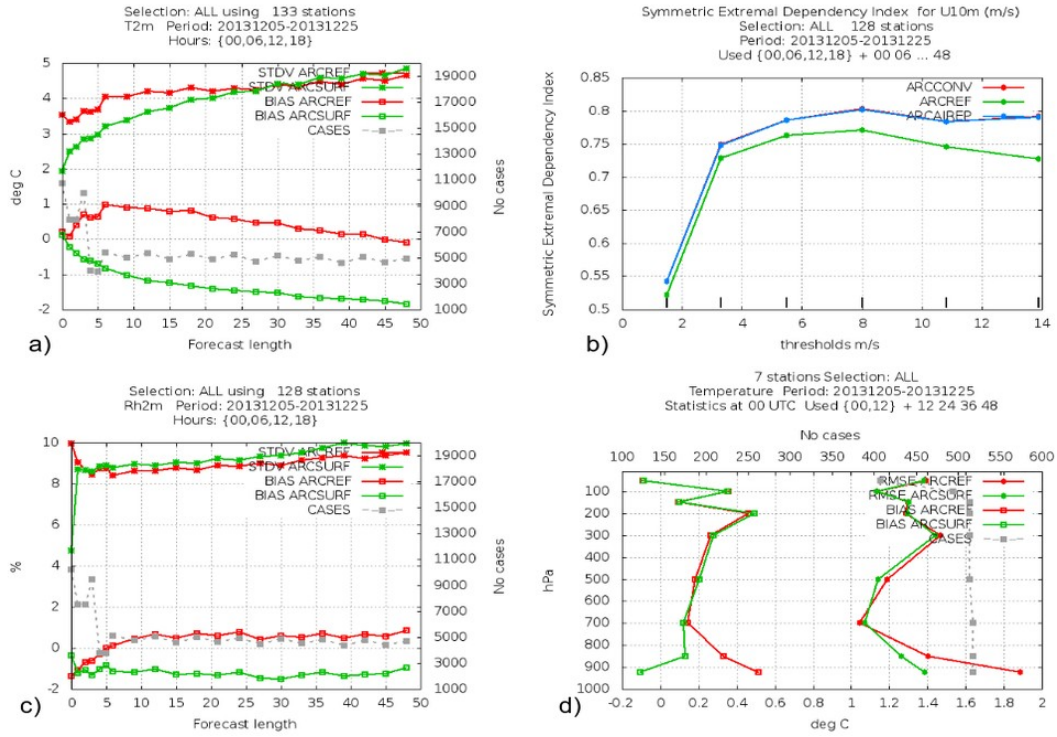

Figures 5. All verifications are against observations. Bias and error standard deviation (STDV) of the 2m temperature (a)) and 2m relative humidity (c)); symmetric extremal dependency index (the higher the index the better the performance – *Christopher et al. 2011*) applied to 10m wind speed (b)); and bias and root-mean-square error (RMSE) of temperature profile (d)).

3- Radiosondes (*Figs. 6*) alone or even with the aircraft data (*Figs. 7*) are not able to improve the performance of the information coming ECMWF model through the "large-scale mixing" procedure (being hydrostatic, but using a lot of observations) over the Arctic. This must be seen on background of the scarceness of radiosondes in the domain.

4- Adding the radiances in the assimilation system clearly shows improvement (*Figs 8*). Here, we start to be closer in quality to the coupling global model ECMWF.

5- The more observations we use the better the accuracy of the forecasts (see the verification profiles against radiosondes in *Fig. 9*). Note that the vertical scores are the mean score over different forecast ranges. See for example the different scores at 700 hPa. In performance quality the best is that of IASI, then that of the humidity sensitive microwave (AMSU-B/MHS), which followed by ATOVN (with both the microwave instruments), then AMSU-A alone with lowest quality shown by run with conventional data only.

6- On *Fig. 10* we can see that one single instrument (instrument groups) can provide pronounced impact, like the case of AMSU-B/MHS during this study period. Fortunately, this impact is also seen very well with the DFS measure, and also supported by the investigation related to the loss of energy in the forecasts with respect to the withdrawn observations from the assimilation system (see Section 3.4.1 for more details).

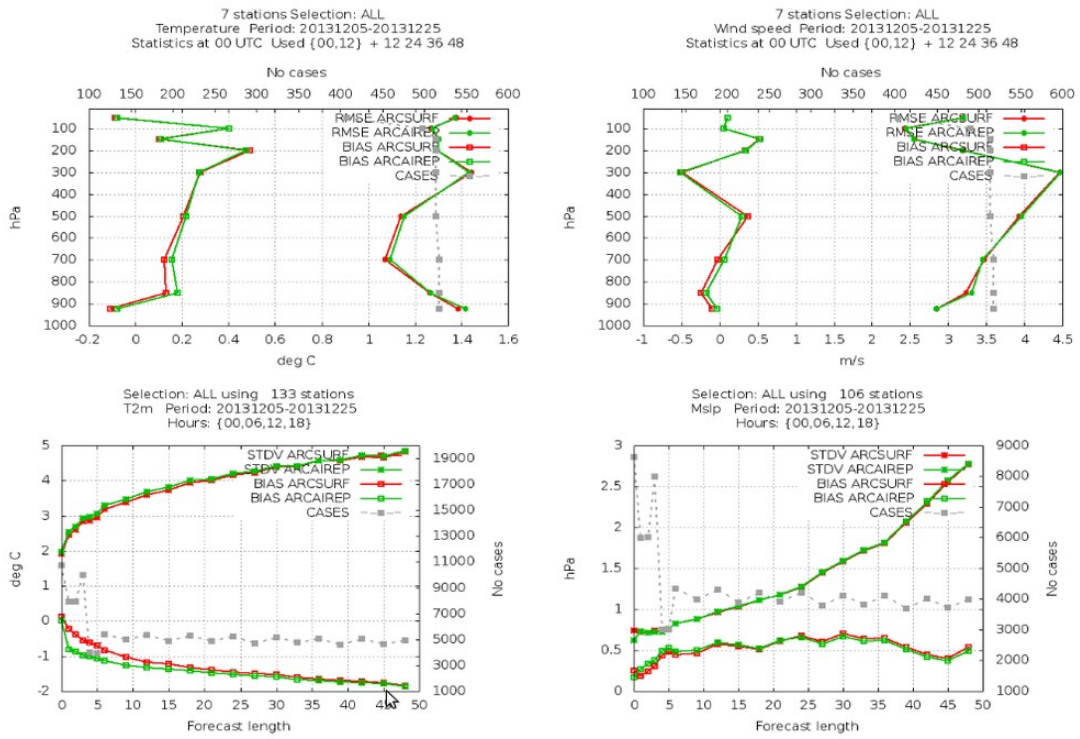

Figures 6. Bias and RMS errors (top plots) of temperature (left) and wind speed (right) comparing runs using surface assimilation only (red line) and run with both assimilation schemes but using only radiosonde data in the upper-air assimilation. The bottom plots show the bias and error STDV for 2m temperature (left) and mean-sea-level pressure (right).

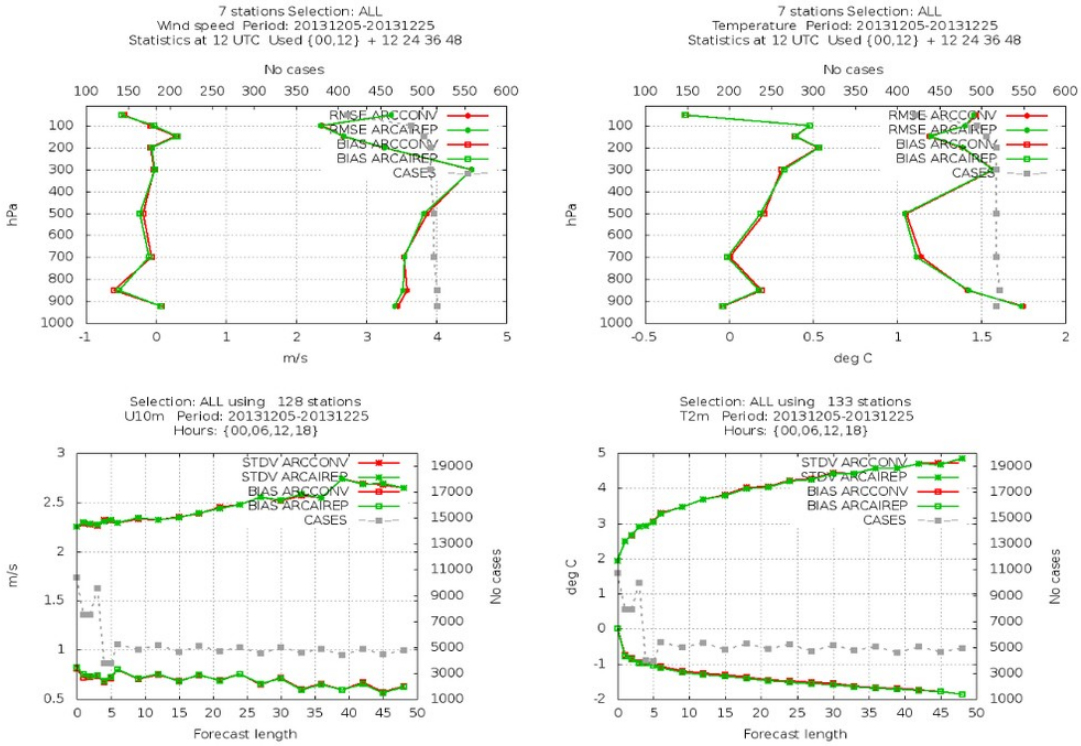

Figures 7. Same as Fig.6, but having different emplacement of figures and different parameters for the bottom plots. And, here we compare the run using radiosonde alone (ARCAIREP) with the one with aircraft data (ARCCONV = radiosonde + aircraft).

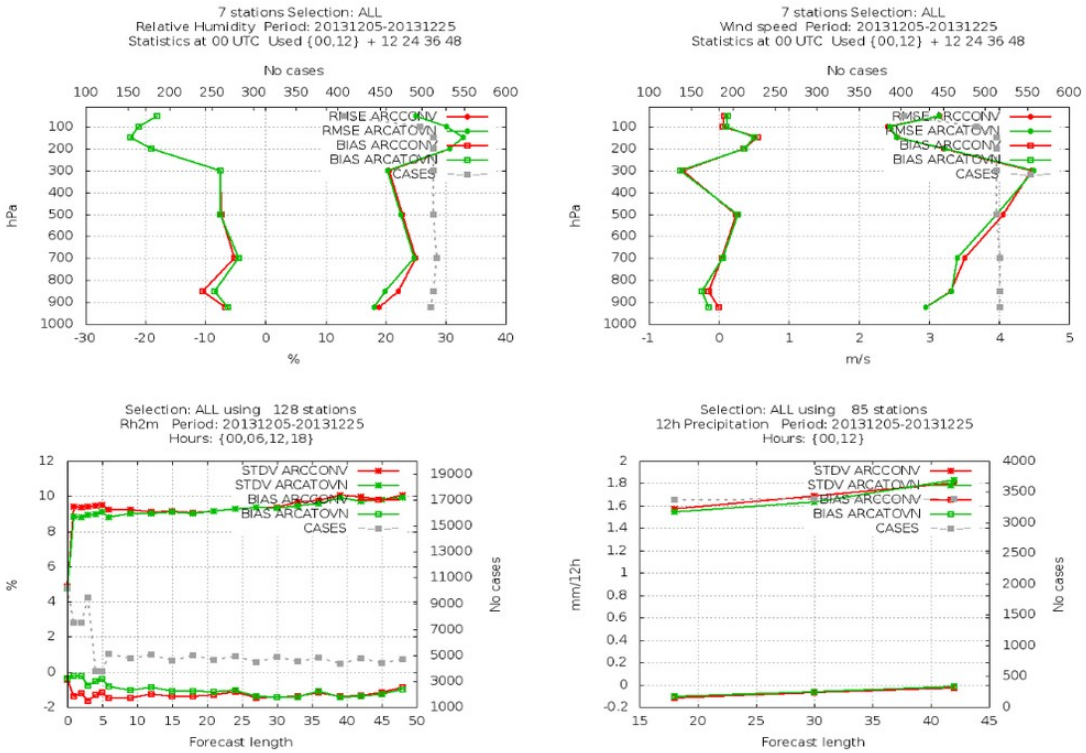

Figures 8. Same as Fig.6, but having different emplacement of figures and different parameters for the bottom plots. Here, we compare the run using ATOVS (AMSU-A and AMSU-B/MHS) with the one with conventional data (ARCCONV = radiosonde + aircraft).

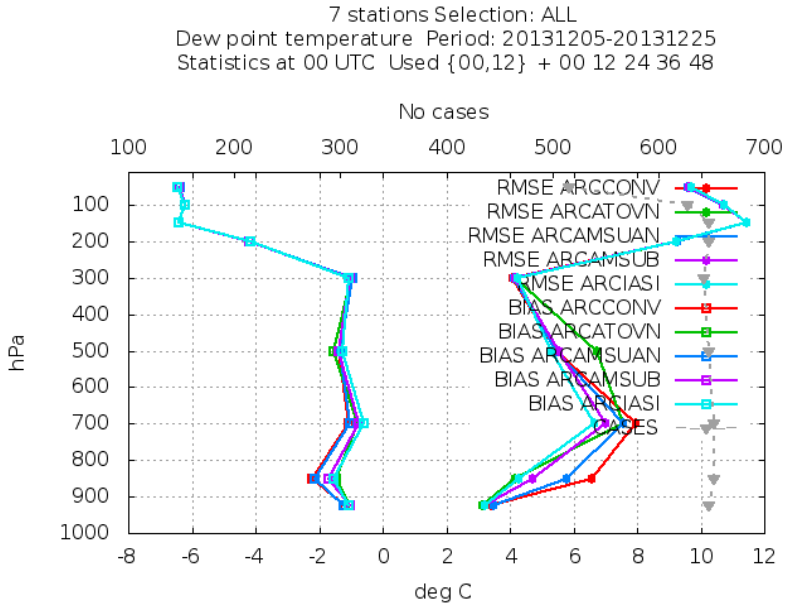

Figure 9. Mean analysis (00, initial state) and forecasts bias and RMS errors for dew point temperature of runs with different observation types.

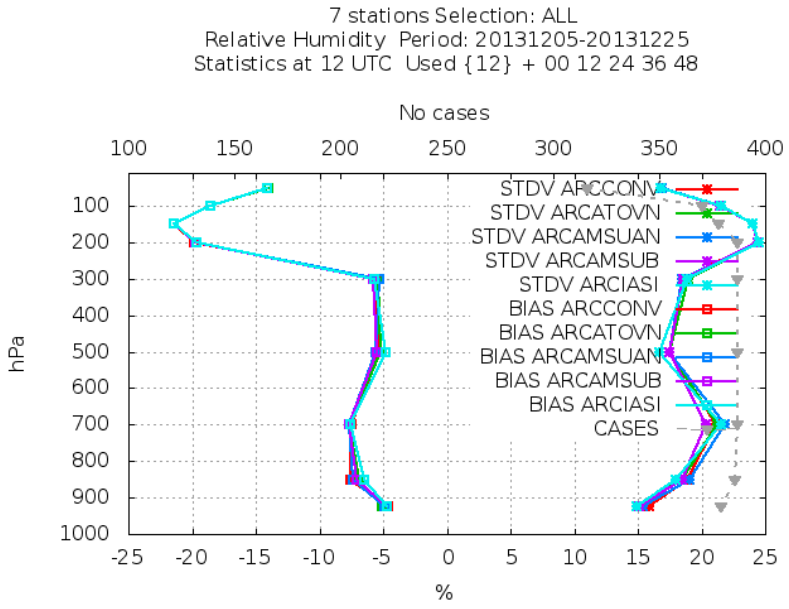

Figure 10. Same as Fig. 9, but for relative humidity and are statistics are for 12 UTC and using only 12 UTC runs.

2.4 Case studies

Two cases low-pressure systems will be highlighted, where one of them – the case of 8th of December 2013 at 12 UTC – is a polar low. The other case – 12th of December 2013 at 00 UTC – is a fast-developing synoptic-scale cyclone passing through the AROME-Arctic domain within a day, day and half.

2.4.1 The polar low case – 08 December 2013

By definition, the polar lows are very intense Arctic (or Antarctic) maritime storms stretching up to 1000 km in diameter and where the surface winds exceed 15 ms^{-1} for part of its existence (*Rasmussen and Turner,* 2003), and on occasion above 30 ms^{-1} (Shapiro *et al.*, 1987). Typically, they last between 12 and 36 hours. As already discussed in our previous study (*Randriamampianina et al,* 2011), and as pointed in Linders and Sætra (2010), "Polar lows are a complex weather phenomenon with hotly debated dynamics. There is not even a generally accepted definition ... ". Shapiro et al. (1987) gave guidance on how the polar lows are "*supposed to develop*", but there are still cases, which do not fully agree with them. Nevertheless, the guidances suggest the existence of an upper-level synoptic-scale disturbance together with the polar low developing at the lower-levels (see Fig. 11, or Randriamampianina et al. (2011) Fig. 13 for more illustration).

In this case, we show the ability of different numerical solutions (with and without data assimilation) in forecasting the state of the polar low at 12 UTC the 8th of December 24 hours ahead.

This polar low developed relatively slowly and lasted quite long after reaching its mature stage (around 00 UTC 9th of December) (see Figs. 12 and 13).

As seen on Fig. 14 all runs predicted a low pressure slightly at different position and with slightly different intensity at the study time. It is worth to mention that the position of the cross-section lines is fixed (very small displacement was done for some cases, if so) for all

forecasts, which may have influence on the cross-sections. Nevertheless, on Fig. 15, we can see that not all the predicted lows have the above described characteristics of a polar low: the near-surface vortex is not clearly seen below 800 hPa.

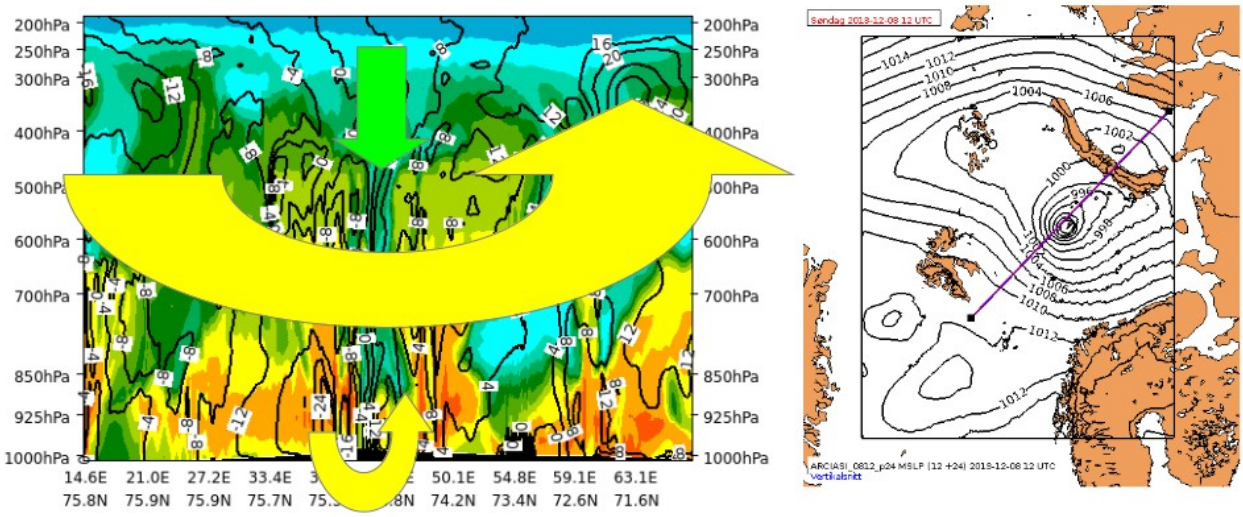

Figure 11. Vertical cross-section of relative humidity (coloured pattern) and a normal-wind field (black lines) along the line shown right hand side map. The larger circle shows the upper-tropospheric synoptic-scale cyclone, and the small one show the polar low (acting below roughly 800 hPa). The cross-section of humidity shows a dry air at the centre of the low as signature of stratospheric air intrusion, as found during the campaign observation (Linders and Sætra, 2010; Kristjánsson *et al*., 2011). The plots are using the forecast using all observations.

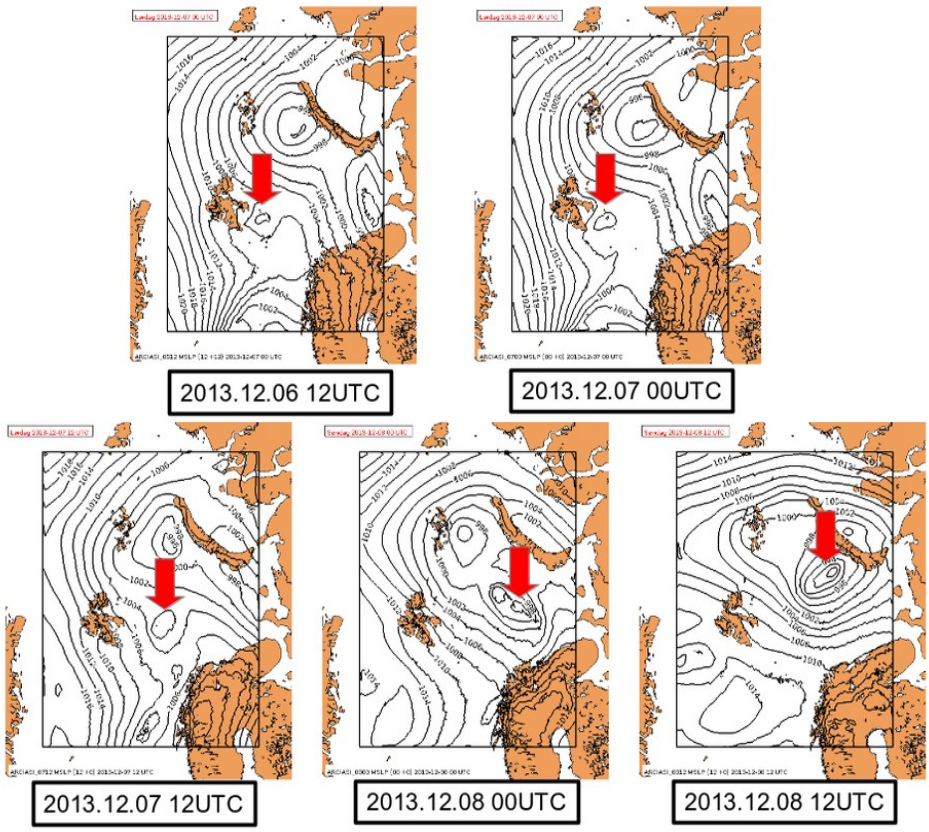

Figure 12. The development of the polar low (pointed with red arrows).

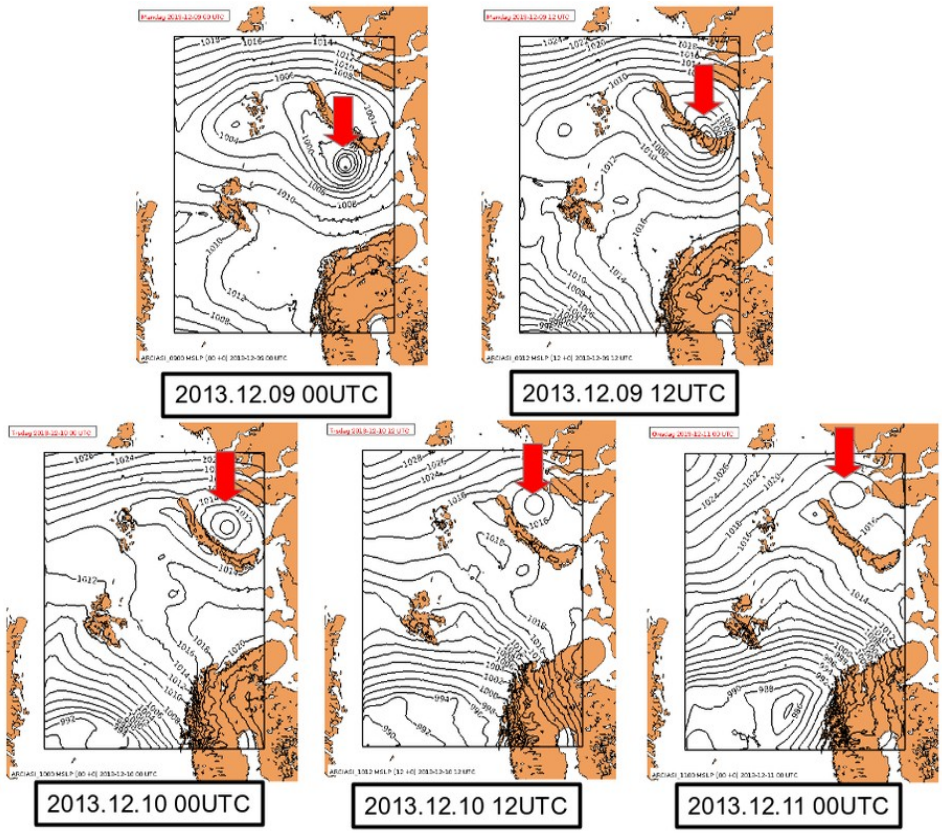

Figure 13. The same as Fig. 12.

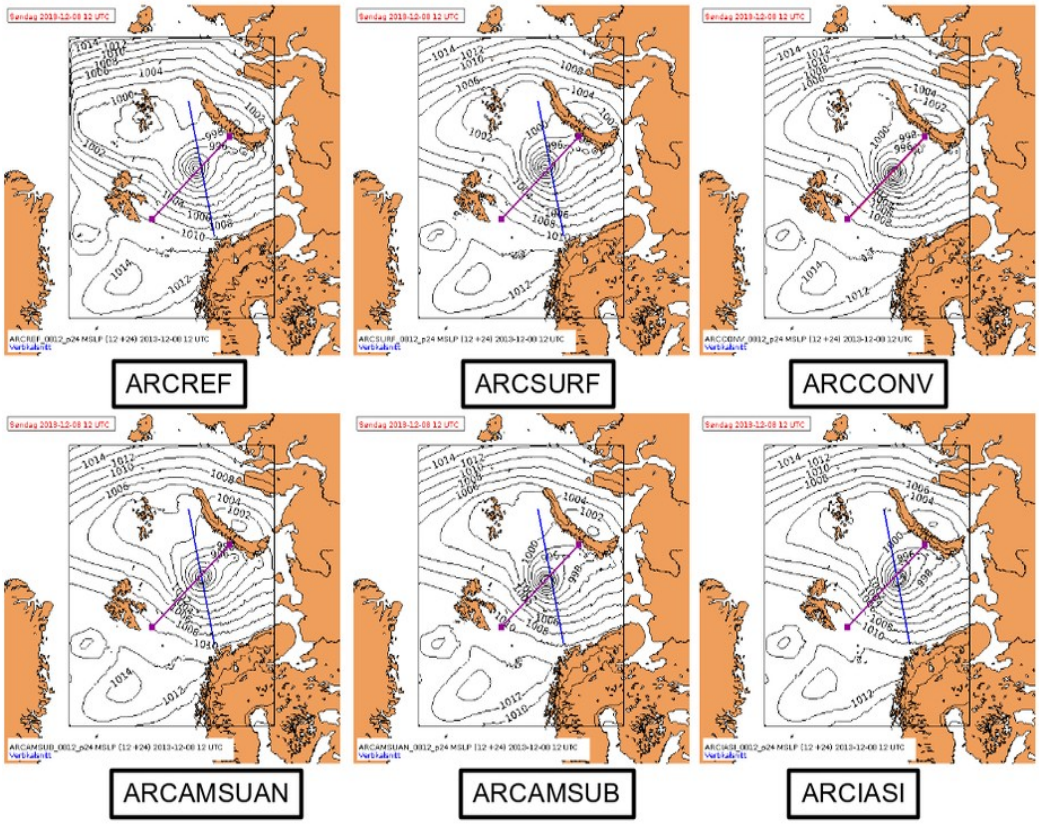

Figure 14. 24-hours forecast of different runs (see experiment's name). The violet lines show the vertical cross-sections shown on Fig. 15.

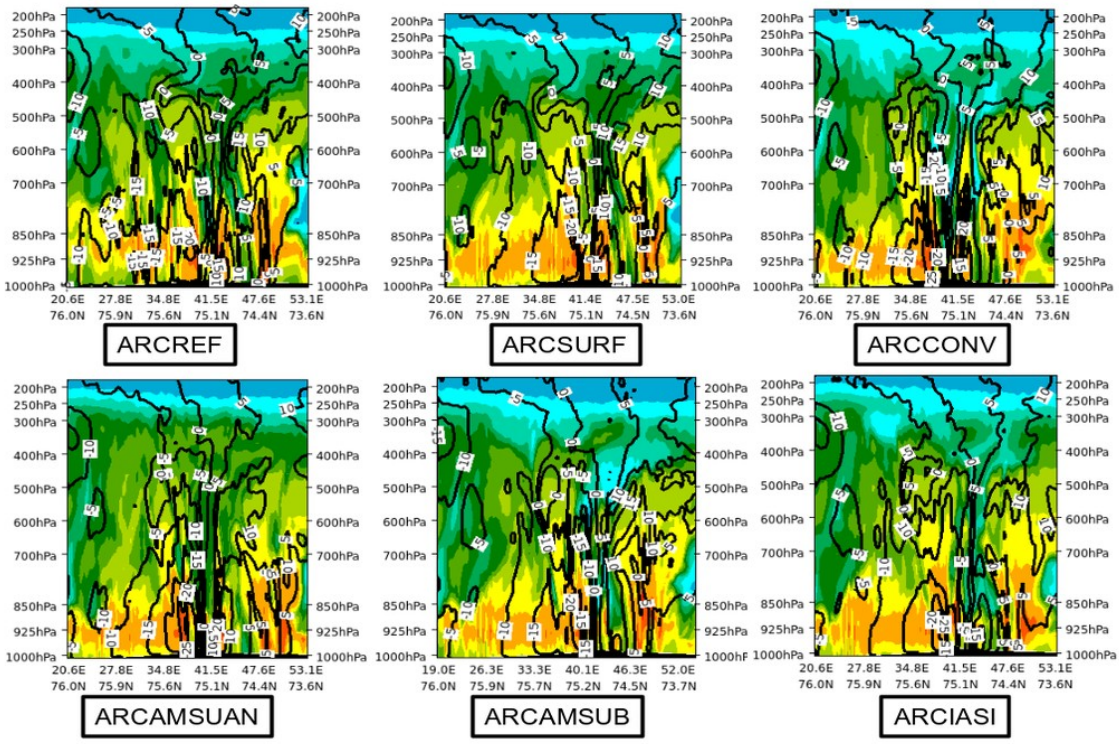

Figure 15. Vertical cross-section of relative humidity and normal-wind field. Cross-section lines are shown on Fig. 14.

2.4.2 A fast moving synoptic-scale cyclone

This case is a fast moving synoptic-scale cyclone entering the domain the 10th of December, developing and go out of the domain 2 days after (*Fig. 16*). It is very interesting to observe that this cyclone is well predicted by each version of the numerical solutions. The forecasts of mean-sea-level pressure (MSLP) look very comparable, even the 36-hours one, which seems to be less accurate (compared to the analyses) than the 48-hour forecasts. But, if we look at the forecast of accumulated precipitation plotted together with 10m wind barbs, then it becomes clearer that the shorter (36-hour) forecast is more accurate. For example, the precipitation along the occlusion front is well forecasted (shown by the red arrow on *Fig. 17*). Furthermore, the performance of different runs is compared in Fig. 18. Even in this short-range forecast, doing only surface assimilation seems to produce less accurate precipitation forecasts than the systems with upper-air data assimilation. Adding radiances in the upper-air assimilation system seems to provide more accurate precipitation forecasts (check also the precipitation inside the red rectangles, Fig. 18).

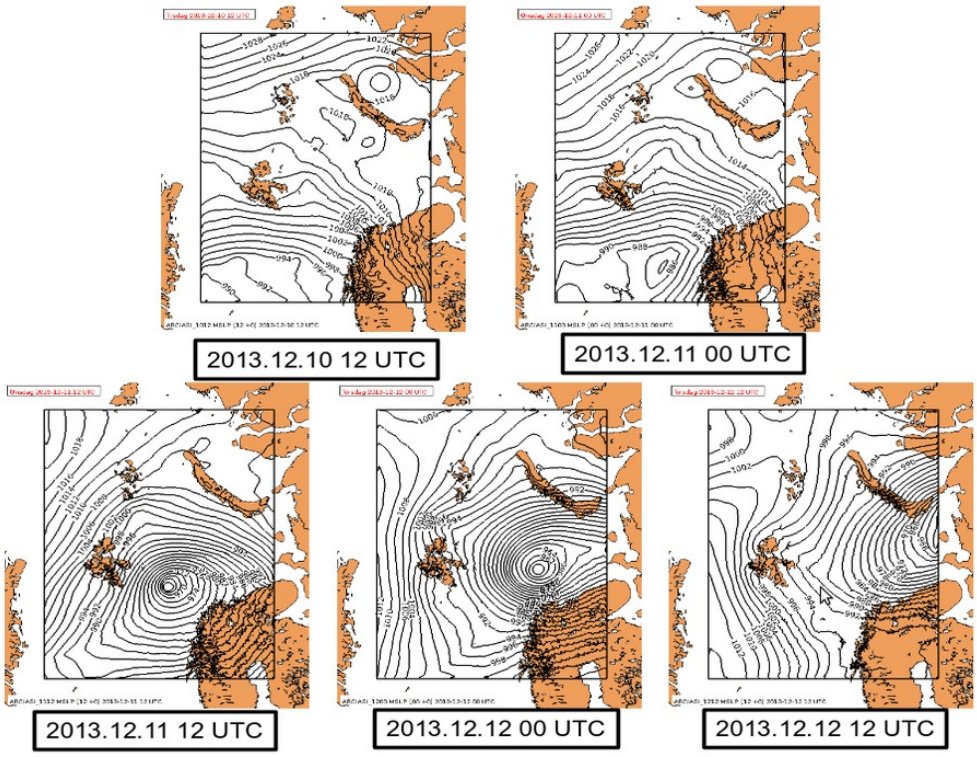

Figure 16. Different analyses describing the fast moving synoptic-scale cyclone

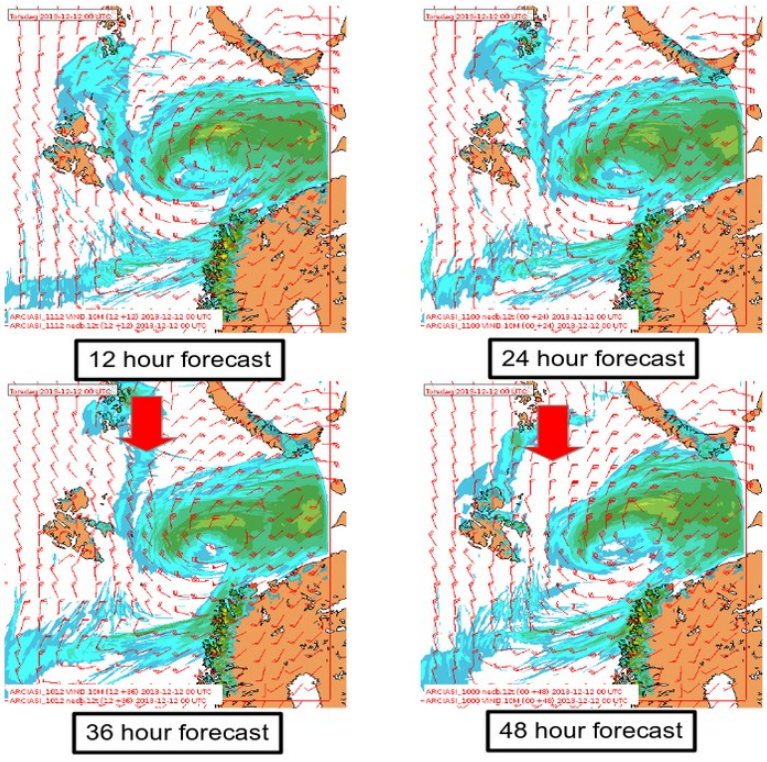

Figure 17. Forecasts of 12-hour accumulated precipitation superposed with 10m wind barbs. Red arrows compare the forecasting of the precipitation along the occlusion front (note also the wind shear).

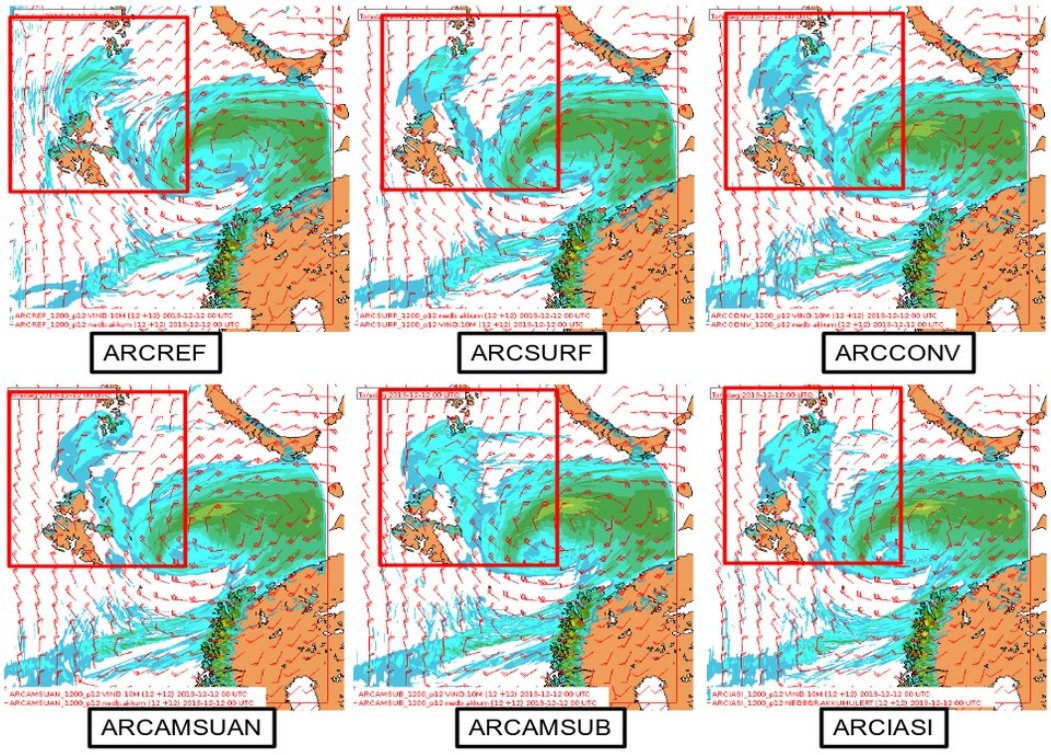

Figure 18. Same as Fig.17, but for different experiments with the same forecast length (12-hour).

2.5.1 The sensitivity of the forecasts to different observations

In the study we use the technique developed by *Storto and Randriamampianina (2010)* to calculate a scalar measure of the impact of different observation types on the forecasts. The sensitivity of the forecast to the observations is defined by the change in a model space-based energy norm, between an experiment with all the observations and as many data-denial experiments as the amount of observing networks to which the forecast sensitivity one wants to be evaluated. The impact of the observations is evaluated by means of a cost function, given as

$$J = \left\langle M_t(\mathbf{x}^{\mathbf{a}}_{\mathbf{ctr}}) - M_t(\mathbf{x}^{\mathbf{a}}_{\mathbf{i}}),\quad M_t(\mathbf{x}^{\mathbf{a}}_{\mathbf{ctr}}) - M_t(\mathbf{x}^{\mathbf{a}}_{\mathbf{i}}) \right\rangle, \qquad (2)$$

where $\mathbf{x}^{\mathbf{a}}_{\mathbf{ctr}}$ and $\mathbf{x}^{\mathbf{a}}_{\mathbf{i}}$ are the analysis from the "all-observation" experiment and that with the withholding of the *i*-th observing group, respectively, M_t is the (fully non-linear) forecast model operator and $\langle \ldots, \ldots \rangle$ stands for the moist total energy norm, defined as in Ehrendorfer *et al.* (1999):

$$\left\langle \mathbf{x}^{\mathbf{i}}_{\mathbf{t}} - \mathbf{x}^{\mathbf{ctr}}_{\mathbf{t}}, \mathbf{x}^{\mathbf{i}}_{\mathbf{t}} - \mathbf{x}^{\mathbf{ctr}}_{\mathbf{t}} \right\rangle = \int_{\eta_0}^{\eta_1}\int_D \left(u^2 + v^2 + \frac{c_p}{T_r}T^2 + \frac{RT_r}{p_r^2}p^2 + \frac{L^2}{c_p T_r}q^2 \right) \frac{\partial p_r}{\partial \eta}\, d\eta\, dD \qquad (3)$$

where u, v, T, p, q being respectively the difference of u- and v-component of wind, temperature, surface pressure and specific humidity between the control forecast and the one without the *i*-th set of observations; c_p, R, L are specific heat at constant pressure, gas constant of dry air, and latent heat condensation; T_r and p_r are reference temperature and reference pressure; η is the vertical coordinate. The previous norm is integrated over all the vertical levels between η_0 and η_1 and over the domain D, which may coincide with the whole model domain depending on the definition of the localisation operator **P**. In our case, for example, the AROME-Arctic domain was divided into four equal sub-domains (*see Fig 19*). This techniques allows us to obtain an indication of the quality loss associated to the withholding of each observation group or parameter from the assimilation system. We

applied this method to evaluate the impact of surface (SYNOP), drifting buoys (DRIBU), aircraft (AIREP), radiosonde (TEMP), used in this study.

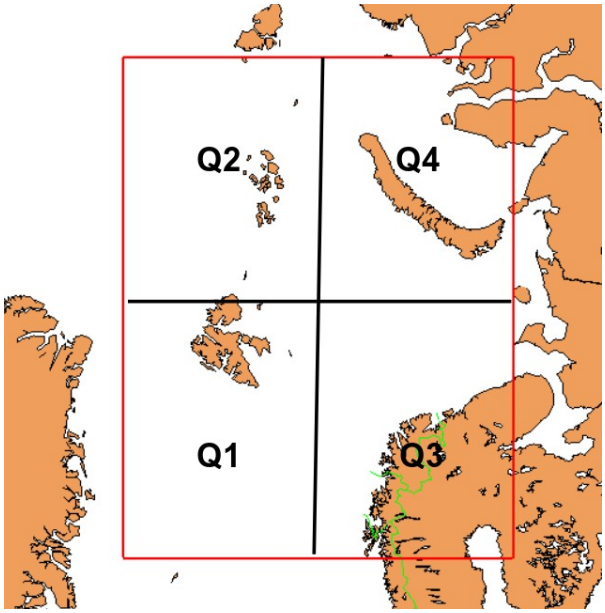

Figure 19. The emplacement of the different quarters inside the AROME-Arctic domain.

Data distant enough apart were used to ensure ergodicity of the initial conditions, as recommended in *Sadiki and Fischer (2005)*. The following dates and time were use: 12 UTC for 06.12.2013 and 15.12.2013, and 00 UTC for 10.12.2013 and 19.12.2013.

The weather conditions along the forecasts at different chosen dates are shown on the *Figs 20-23.*

The sensitivity of the AROME-Arctic forecast to different observations depends on the weather phenomenon actually occupying the domain as a whole (total norm). Separate computation of the moist energy norms for different quarters of the domain shows that forecasting of sensitive systems (like for example polar low – see the case of 06 of December or the case of 12th). Note that the weather conditions in first half of the study period was more influenced by different kinds of polar vortices than the second one. This particular change of dominating weather regime can be seen in the relative sensitivity of the forecast system for the two last dates (15th and 19th of December). The sensitivity of different length of forecast to different observation types was estimated. Here, we highlight only few of them – 6-hour, 12-hour and 48-hour forecasts (Figs 24, 25, 26, respectively). We can see that diffenrent type of observations play important role for certain weather regime. But, again, IASI and AMSU-B radiances seem to be the most influencing observations.

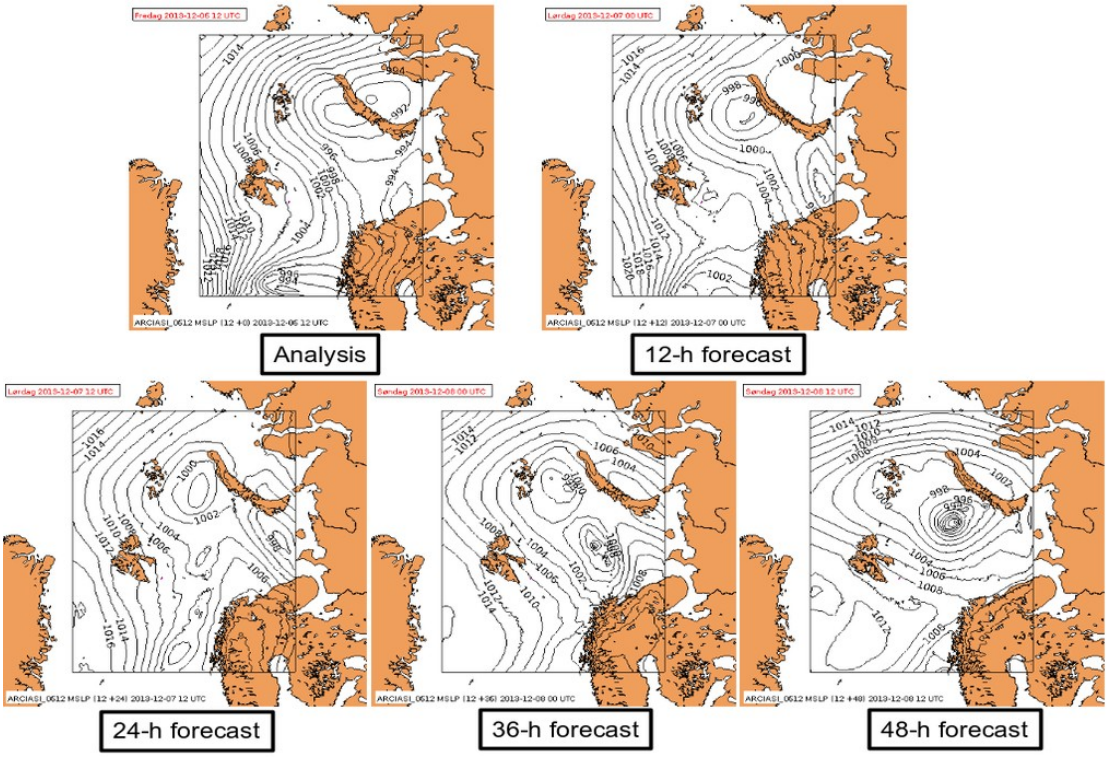

Figure 20. The analysis and forecast from 6th of December 2013 12 UTC.

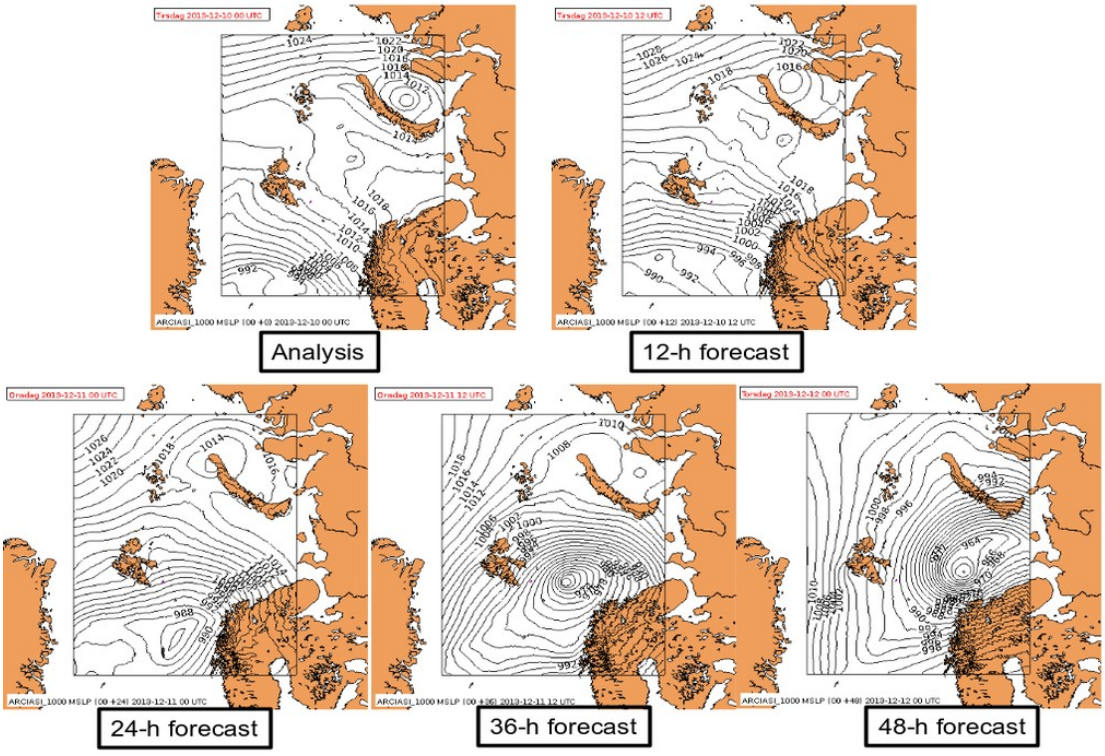

Figure 21. Same a Fig. 20, but for 10th of December 2013 00 UTC.

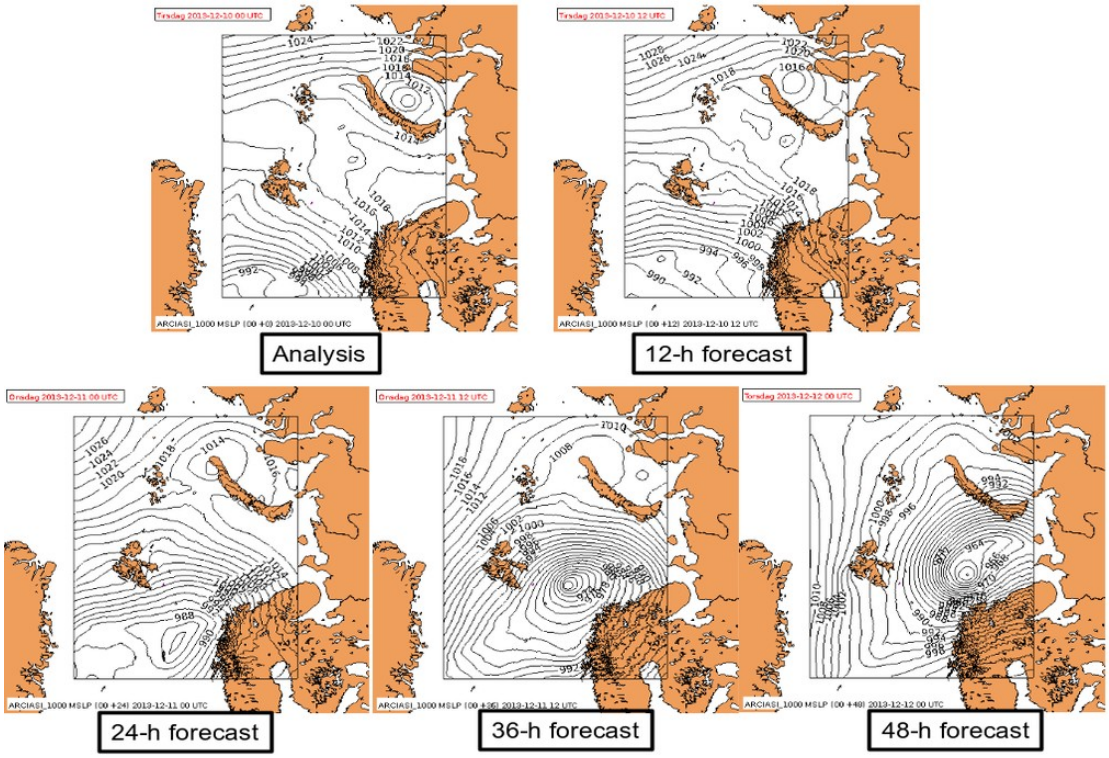

Figure 22. Same as Fig.20, but for 15th of December 2013 12 UTC.

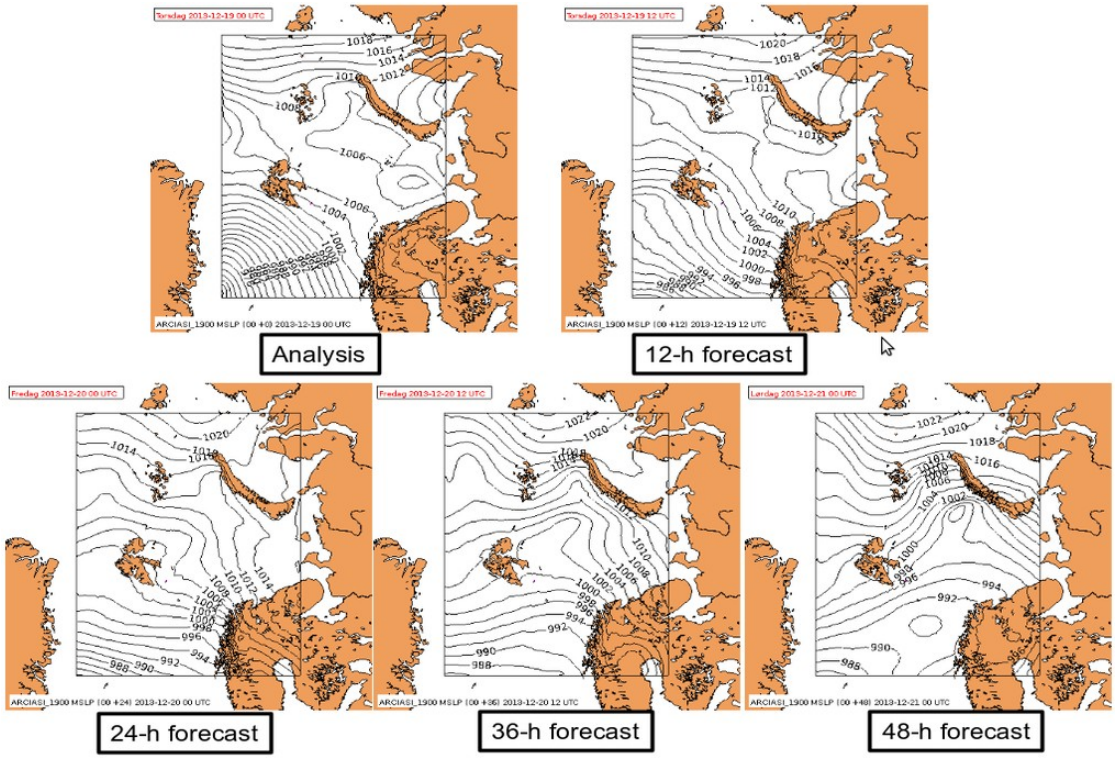

Figure 23. Same as Fig.20, but for 19th of December 2013 00 UTC.

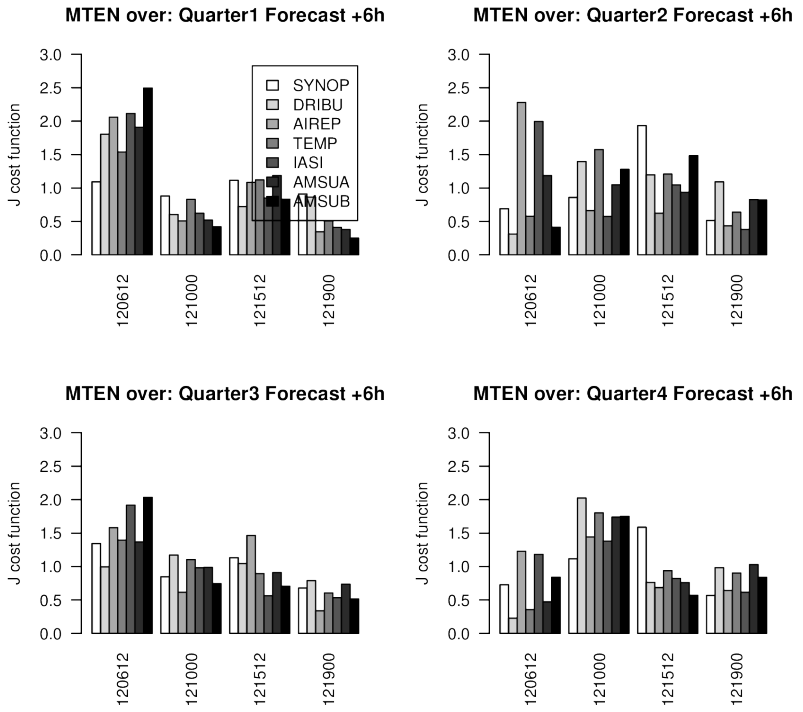

Figure 24. The sensitivity of the AROME-Arctic 6-hour forecast to different observations at different dates and quarters of the model domain (*see also Fig. 19*).

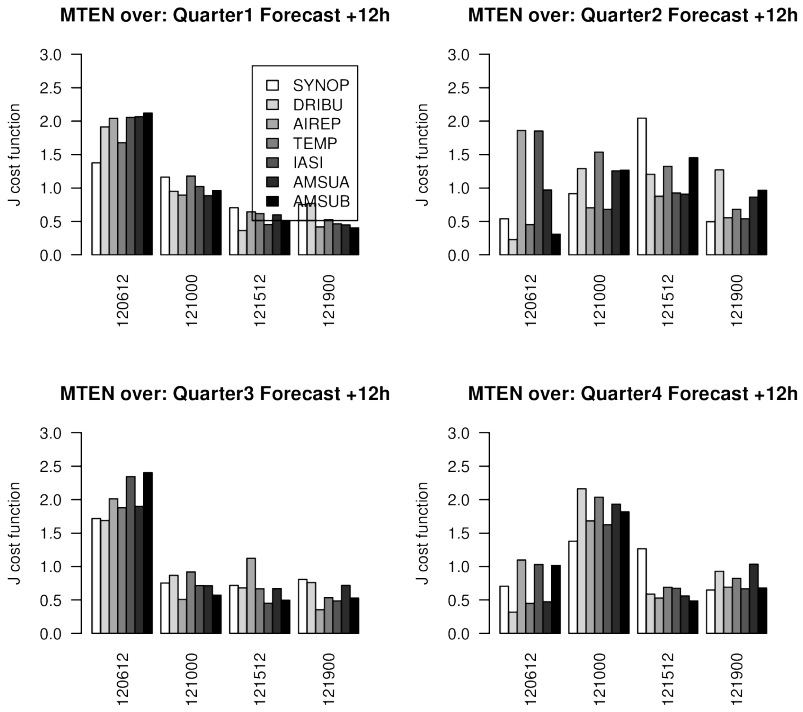

Figure 25. Same as Fig. 24, but for 12-hour forecasts.

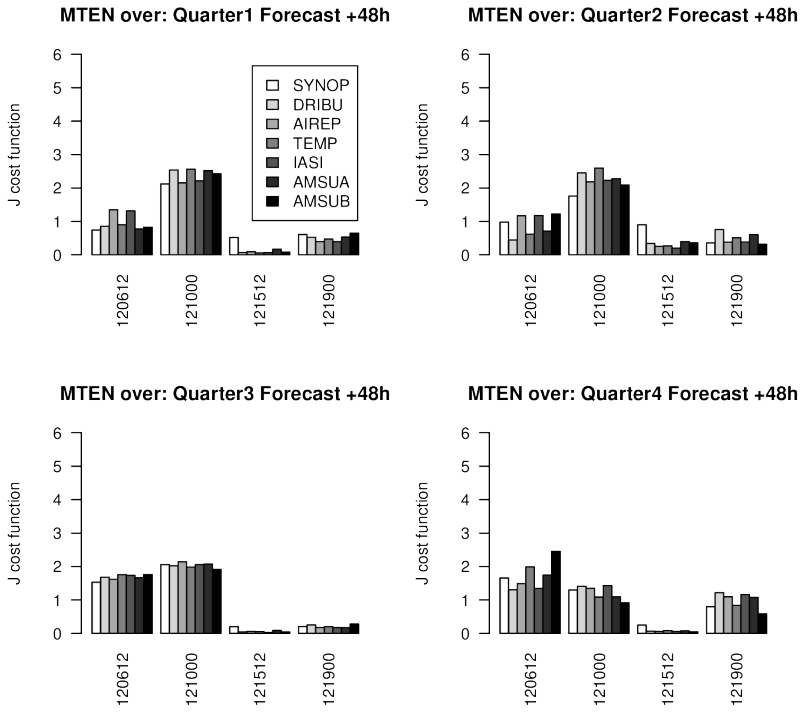

Figure 26. Same as Fig. 24, but for 48-hour forecasts.

3 Observing system simulation experiments (OSSE)

In the final part of this work, we have implemented a system for Observing System Simulation Experiments (OSSE) with the aim to provide guidance and recommendations for key areas to improve the monitoring and forecasting capabilities and quantify the expected improvements. The experiments with the observation system usage done earlier in this report could only assess impact of already existing parts of the observing system. The present OSSE method is designed to investigate the potential impact of current *or future* observing systems in an observation simulation approach [see for instance Masutani et al., 2010]. It is based on data assimilation ideas and simulated rather than real observations are the input to the system. Simulated observations are produced from a reference atmospheric state, called the Nature Run (NR) and an estimate of observation error value is added to make them more realistic. Finally, resulting synthetic observations are ingested into the Data Assimilation System (DAS) using comparable characteristics than the operational one. The Analysis and forecast outputs are then compared to perform the impacts study.

Here, the global Action de Recherche Petite Echelle Grande Echelle (ARPEGE) system is used, in forecast mode, to compute the NR during 3 months in summer 2013 (June to September). This model was employed because it is a mature Numerical Weather Prediction (NWP) system with demonstrated forecast skill. The simulated fields are extracted every hour for both prognostic and diagnostic model variables. The NR is the source of the full "perfect" observation dataset (conventional and satellites).

Some appropriate amount of noise, with statistical properties corresponding to realistic observation errors, is added to the simulated observations to make them more realistic. In fact, if the error is indeed appropriate, then the impact of simulated observation on an OSSE will be similar to the impact that real-world observations had on operational assimilation (*Masutani et al., 2010*). When the system is well calibrated, simulated observations are assimilated into the Experimental AROME-Arctic.

3.1 Observations, models and Methodology

3.1.1 Conventional measurements and Satellite radiances

The coverage and characteristics of the various components of the Arctic observing system is summarized in this section (more details can be found in Schyberg et al., 2013).

Available observations include radiosonde and SYNOP measurements as well as buoys, aircraft and satellite. The SYNOP data usually provides pressure, temperature and moisture information, mainly over land surfaces. Drifting buoys and ships measures pressure, and sometimes also air and sea temperatures. From the surface up to the stratosphere, radiosondes inform on temperature, wind and moisture and aircraft usually provide the same measurements at ight level near airports. In general, conventional observing systems provide very sparse atmospheric information and large parts of the ice sheet remains uncovered but this is compensated by data from satellite sounding instruments.

Available satellite observations include 2 AMSU sensors from NOAA and Metop satellites, 1 interferometric infrared sounding sensors (IASI) from Metop. Information on upper-air temperature, humidity and wind can be retrieved from radiances with a very good coverage (in space and time).

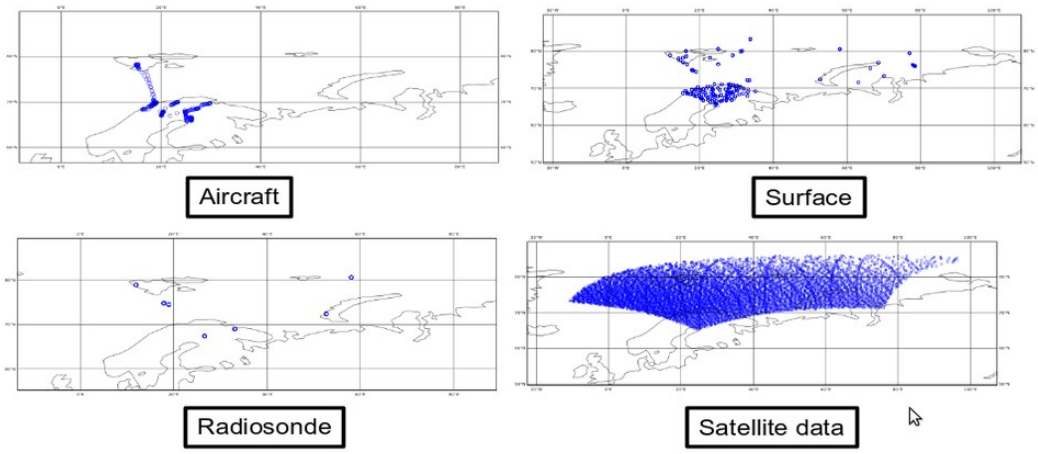

Figure 27. Maps of Observation coverage over the Arctic area, 20120804 at 12 UTC.

3.1.2 The ARPEGE Nature Run

The global ARPEGE system is used to compute the "true" state of the atmosphere, called the Nature Run (NR). The ARPEGE system is used operationally in Meteo-France for NWP since 1992. The code is derived from the Integrated Forecasting System (IFS)/ARPEGE software and it is used to create the NR which is a long, in interrupted forecast representing the "true" state of the atmosphere. ARPEGE is a global spectral model, with a Gaussian grid for the grid-point calculations. The vertical discretisation is done according a following-terrain pressure hybrid coordinate over 105 vertical levels (from 0.1hPa to 10m). The version used to create the ARPEGE-NR has the new horizontal resolution TI1198 with stretching factor 2.2 (around 7.5km over France and 36km over antipodes). This NWP model was employed because it is a mature system with demonstrated forecast skill.

The ARPEGE-NR was produced using ARPEGE in a forecast mode. The simulated fields are available every hour for both prognostic and diagnostic model fields.

The period covers 2 months in winter 2013 (February to March) and 4 months in summer 2013 (June to September). The first guess is based on one atmospheric analysis produced

by the operational ARPEGE system. A few weeks after the simulation begin, the atmospheric state of the ARPEGE-NR diverges from the one of ARPEGE.

Assimilated observations influence held in the first guess is progressively eradicated and the system converges toward climatologies, evolving continuously in a dynamically consistent way. Figure 28 and 29 give an example of specific humidity and temperature fields produced by the Nature Run.

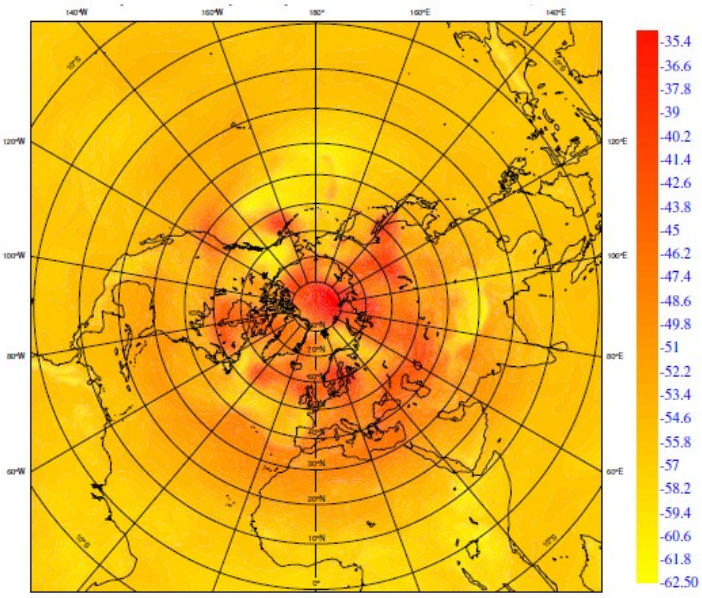

Figure 28. Maps of Temperature (oC) from ARPEGE the Nature Run over the Northern Hemisphere, at 850 hPa,2013/07/23-00UTC.

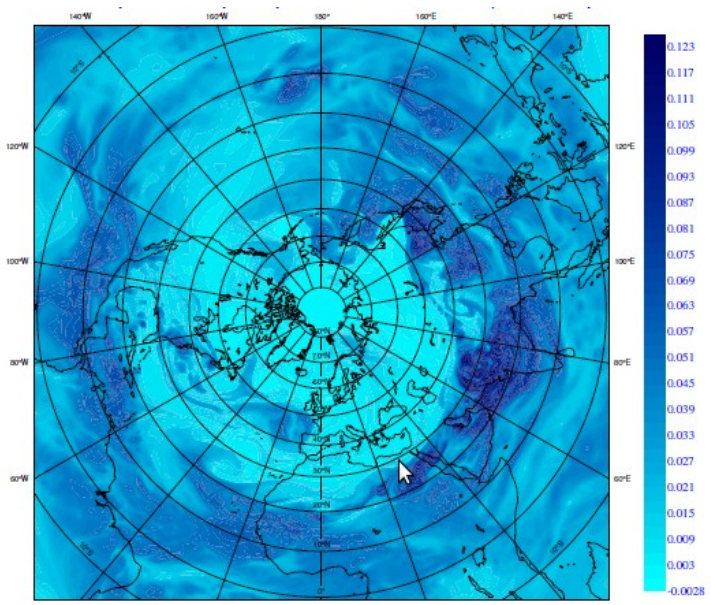

Figure 28. Maps of Specific Humidity (g/kg) from the ARPEGE Nature Run over the Northern Hemisphere, at 850 hPa,2013/07/23-00UTC.

3.1.2 Method and OSSE configurations

The ARPEGE-NR was useful for many applications within the OSSE framework (*Fig. 29*). First, it is the source of simulated observations. To simulate perfect conventional observations, it is only necessary to locate the observation type to be simulated in the space

and time coordinate of the background field (i.e. the NR). The radiative transfer model (RTTOV-10) was used additionally to simulate radiance observations.

The presence of clouds were not considered in this study. Perfect observations are assumed unbiased (The VarBC scheme is turned off). To make simulations more realistic and take account for observation errors, a Gaussian perturbation is explicitly added to the simulated values. The amplitude of the perturbation is scaled using the observation error standard deviation (σo), as specified in the operational model, as well as a coefficient. This coefficient permits to scale errors independently for each observation type (radiance, aircraft, buyos ...).

Since the nature run might does no mimic exactly the true atmosphere, the model "errors" might be different from when comparing to the real atmosphere, and to get even more realistic results it makes sense to do a system calibration. This calibration aims to verify the simulated data impact by comparing it to real data impact. If errors are well estimated, data impact of existing instrument is comparable to their impact in the OSSE. To ensure that errors in the OSSE describe the same statistics than the real world assimilation, one can compare innovations (y-H (x)) in both experiments. y is the observation, H (x) is the observation operator used to generate the best estimate for the observation value. Distribution of differences in Observation minus Background (OmB) and in Observation minus Analysis (OmA) should be the similar in the both OSSE and real world data assimilation experiments (as in the OSEs presented in previous sections).

To perform this task, observations were simulated repeatedly with various conditions and error assignments during 10 days. Several coefficients were tested (0.2, 0.4, 0.6, 0.8, 1, 1.2). Then, numerous manual modications of σo were changed for specific observations, vertical levels, channels ...

Figure 30 shows an example of the method used for the calibration. Specified values of standard deviation and OmA statistics are presented. The objective of the calibration is to t as close as possible to the real world statistic (red curve). One can note that if σosse = σoper and alfa=1, the differences between OmA configurations is large,especially under 750 hPa (figure 1). For humidity radiosonde data, the best results are obtained for = 0:5 (i.e. σoper/2) plus various manual adaptations for levels in 900 and 950 hPa.

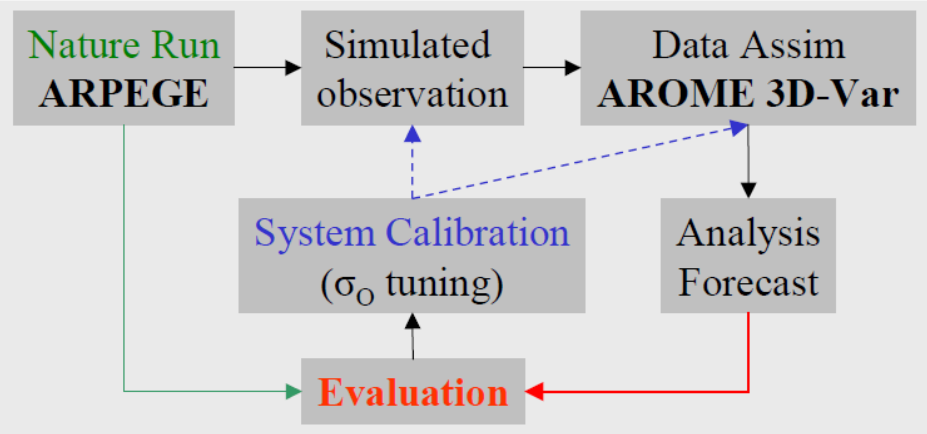

Figure 29. Observing System Simulation Experiment (OSSE) scheme.

When the statistic properties of the analysis increment for the OSSE and the real world assimilation are close enough, the Control (CTL) run is computed. The initial condition and boundary conditions are generated by interpolation from the NR. Atmospheric fields were not perturbed. The configuration E927, included in the Fullpos package, is used to change geometry and resolution (from ARPEGE to HARMONIE).

Surface parameters are initialized with a climatology. Surface elds are coupled with the atmosphere and propagated in time by a 3h-forecast. Any observation are assimilated into

the surface module. The CTL run for the OSSE experiment was performed during the summer: August 2013. Simulated observations were produced for the same period over the Arctic domain, and assimilated in the CTL run. The HARMONIE 3D-Var produces one atmospheric analysis every 3h to be used as initial condition for 24/48h-forecast. Modifications of the observation network and addition of new observations are then possible to be tested in the OSSE framework. The ARPEGE-NR is used to evaluate the quality of the produced analysis and the forecast skills when the new observing system is included or not.

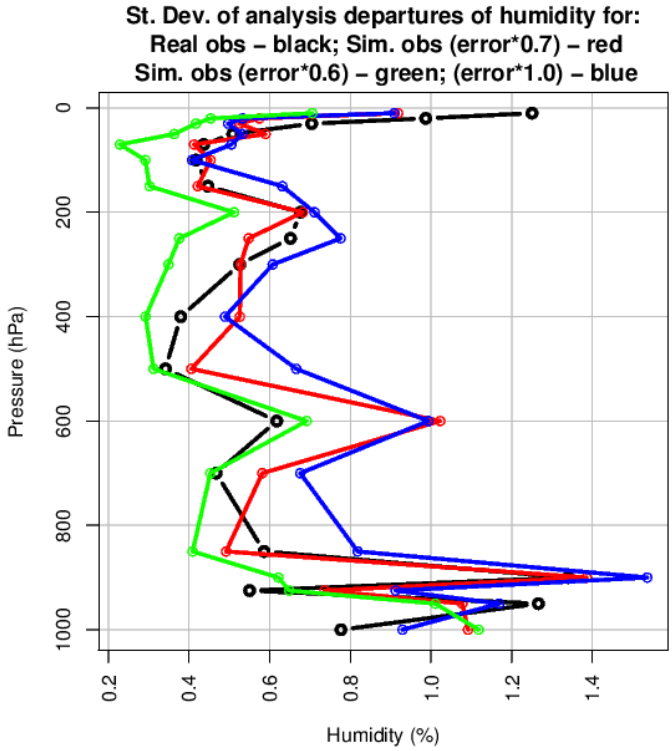

Figure 30. Example of simulation/tuning of the observation error for the radiosonde temperature.

3.2 Network extension and future observation scenario experimentation

All important present components of the observing system can be simulated in this framework, which is necessary to do since we want to assess addons or extensions to the present observing system. We want to see how these extensions can be complementary and fill gaps in the existing observation coverage.

We have determined that the tuning value “alfa” is 0.7 with slight manual adjustments, which OSSE system ready for assessment of future scenarios.

For the definition of a set of future observing scenarios we have not looked at future satellite programmes, which have a long planning horizon and are expensive cooperative programmes typically planned in a global framework by satellite agencies such as EUMETSAT and NOAA. We have chosen to focus on some options for extending the conventional network of observations. This requires more local infrastructure, and it could be seen as feasible economically if some cooperative frame can be set up for this.

We have proposed to options for the OSSE simulations of extensions. First, nn top of the available type of observations, we propose to simulate a multiple number of drifting buoys (measureing surface pressure) relative to today. A scenario with roughly 3 times more that the currently available is shown in Fig. 31.

A second extension which could be performed without too high requirements on extra infrastructure could be to simulate extended frequencey of radiosonde launches relative to

today. Most existing radiosondes in the area only launch 1-2 times per 24 hours. We plan to simulate multiple launches (4 times a day per station) from the existing radiosonde stations.

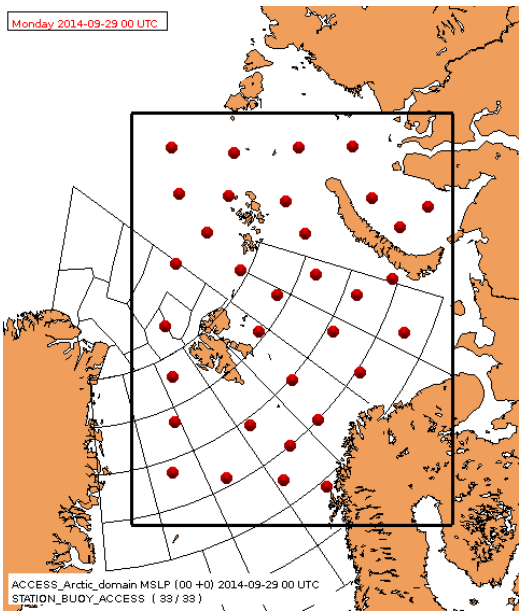

Figure 31. The planned random position of drifting buoys over the AROME-Arctic domain.

4 Concluding remarks

We have observed the fact that NWP forecast quality is lower in the Arctic than in the regions further south and earlier research has indicated that a factor behind this is the composition of the observing system in the Arctic, in particular the scarceness of conventional observations.

To further assess possible strategies for alleviating the situation and propose scenarios for a future Arctic observing system, we have performed a set of experiments to gain a more detailed insight than before in the contributions of the components of the present observing system in a regional state-of-the-art non-hydrostatic NWP model. These observing system experiments have been evaluted both in terms of a measure of the information content of observations with respect to analysis quality and with respect to the impact on forecasts assesed (a) through case studies, (b) through a norm measuring the impact on forecasts and (c) through the quality of forecasts verified with available reference observations.

The studies show that conventional observations can play an important role in correcting the surface state of the model, but verify that the present upper-air conventional observations in the area are to scarce to have a significant effect on forecasts. We demonstrate that present satellite sounding data already is an important player in providing quality to forecasts at present. This is the case with satellite temperature sounding data, and we found here also that satellite moisture sounding data plays a very important role. This impact of moisture observations is slightly surprising and interesting.

This clearly highlights that satellite information will be important also in the future evolution of the Arctic observing system, and that efforts to enhance the extraction of information from satellite is a key area. We also find scenarios enhancing the conventional observing system beyond the limited impact we find today, interesting. Options which could be logisitcally and economically feasible could be to increase the launch frequency of the few radiosonde stations in the region, and also to increase the number of drifting surface buoys measuring pressure in the area.

To quantify further the impacts of these strategies, we have implemented and performed necessary tuning of an Observing System Simulation framework with the same limited-area NWP system. Proposed scenarios to be evaluted in more detail includes both enhanced

exploitation of satellite data and more frequent radiosonde launches as well as higher density of drifting pressure buoys.

Web references

1- ECMWF web portal: http://www.ecmwf.int/en/forecasts/documentation-and-support

2- ALADIN web portal: http://www.cnrm.meteo.fr/aladin/

3- HIRLAM web portal: http://www.hirlam.org/

Literature references

Auligné T, McNally AP, Dee DP. 2007. Adaptive bias correction for satellite data in a numerical weather prediction system. Q. J. R. Meteorol. Soc. 133: 631–642.

Cardinali C, Pezzulli S, Andersson E. 2004. Influence-matrix diagnostic of a data assimilation system. Q. J. R. Meteorol. Soc. 130: 2767–2786.

Chapnik B, Desroziers G, Rabier F, Talagrand O. 2006. Diagnosis and tuning of observational error in a quasi-operational data assimilation setting. Q. J. R. Meteorol. Soc. 132: 543–565.

Christopher A., T. Ferro and David B. Stephenson, 2011: Extremal Dependence Indices: Improved Verification Measures for Deterministic Forecasts of Rare Binary Events. Wea. Forecasting, 26, 699–713

Clough, S. A., M. J. Iacono, J.-L. Moncet, Line-by-line calculations of atmospheric fluxes and cooling rates: Application to water vapor, J. Geophys. Res., 97, 15761–15785, 1992.

Clough, S.A., M.W. Shephard, E.J. Mlawer, J.S. Delamere, M.J. Iacono, K. Cady-Pereira, S. Boukabara, P.D. Brown, Atmospheric Radiative Transfer Modeling: a Summary of the AER Codes, J. Quant. Spectrosc. Radiat. Transfer, 91, 233-244, 2005.

Ehrendorfer M, Errico RM, Raeder KD. 1999. Singular-vector perturbation growth in a primitive equation model with moist physics. J. Atmos. Sci. 56: 1627–1648.

Kristjánsson JE, Barstad I, Aspelien T, Føre I, Hov Ø, Irvine E, Iversen T, Kolstad E, Nordeng TE, McInnes H, Randriamampianina R, Sætra Ø, Ólafsson H, Shapiro M, Spengler T. 2011. The Norwegian IPY-THORPEX: Polar lows and Arctic fronts during the 2008 Andøya campaign. Bull. Amer. Meteor. Soc., **92**, 1443–1466.

Linders T, Sætra Ø. 2010. Can CAPE maintain polar lows? J. Atmos. Sci. 67: 2559–2571.

Lindskog M, Dahlbom M, Thorsteinsson S, Dahlgren P, Randriamampianina R, Bojarova J, 2012: ATOVS Processing and Usage in the HARMONIE Reference System. HIRLAM Newsletter 59: 33-43, available via http://www.hirlam.org.

Masutani M, Woollen JS, Lord SJ, Emmitt GD, Kleespies TJ, Wood SA, Greco S, Sun H, Terry J, Kapoor V, Treadon RE, Campana KA. 2010. Observing system simulation experiments at the National Centers for Environmental Prediction. J. Geophys. Res. 115.

Matricardi M, Chevallier F, Kelly G, Thépaut J-N. 2004. An improved general fast radiative transfer model for the assimilation of radiance observations. Q. J. R. Meteorol. Soc. 130: 153–173.

Montmerle T, Rabier F, Fischer C. 2007. Relative impact of polar-orbiting and geostationary satellite radiances in the Aladin/France numerical weather prediction system. Q. J. R. Meteorol. Soc. 133: 655–671.

Rabier F, Fourrié N, Chafaï D, Prunet P. 2002. Channel selection methods for Infrared Atmospheric Sounding Interferometer radiances. Q. J. R. Meteorol. Soc. 128: 1011–1027.

Randriamampianina R. 2006. Impact of high resolution satellite observations in the ALADIN/HU model. Idöjárás 110: 329–347.

Randriamampianina R, Iversen T, Storto A. 2011. Exploring the assimilation of IASI radiances in forecasting polar lows. Q. J. R. Meteorol. Soc. 137, pp. 1674–1687, October 2011.

Rasmussen EA, Turner J (eds). 2003. Polar Lows. Cambridge University Press.

Sadiki, W. and Fischer, C. 2005 A posteriori validation applied to the 3D-Var Arp`ege and Aladin data assimilation systems. Tellus, 57A, 21–34

Schyberg, H., T. Nipen and R. Randriamampianina, 2013: Arctic forecast quality and assessment of state and impacts of the components of the Arctic observing system. ACCESS Deliverable report D1.81, September 2013.

Seity, Y., P. Brousseau, S. Malardel, G. Hello, P. Bénard, F. Bouttier, C. Lac, V. Masson, 2011: The AROME-France Convective-Scale Operational Model. Mon. Wea. Rev., 139, 976–991.

Shapiro MA, Fedor LS, Hampel T. 1987. Research aircraft measurements of a polar low over the Norwegian Sea. Tellus 39A: 272–306.

Storto A, Randriamampianina R. 2010: A new bias correction scheme for assimilating GPS zenith tropospheric delay estimates. Idöjárás 114: 237–250.

Vignes O., 2011: A simple strategy to take advantage of boundary (ECMWF) forecast quality in Harmonie 3D-Var cycling. Available on the Hirlam web portal (access available on December 2014): https://hirlam.org/trac/attachment/wiki/HarmonieSystemDocumentation/lsmixbc.ppt.